DECEMBER 2023 M.Sc. in Optic and Acoustic Engineering SERDAR ŞENGÜL

REPUBLIC OF TÜRKİYE

GAZİANTEP UNIVERSITY

GRADUATE SCHOOL OF NATURAL & APPLIED SCIENCES

DESIGN AND FABRICATION OF HIGH-POWER LASER DIODE BAR

M.Sc. THESIS

IN

OPTIC AND ACOUSTIC ENGINEERING

BY

SERDAR ŞENGÜL

DECEMBER 2023

DESIGN AND FABRICATION OF HIGH-POWER LASER DIODE BAR

M.Sc. Thesis

in

Optic and Acoustic Engineering

Gaziantep University

Supervisor

Prof. Dr. Ahmet BİNGÜL

Co-Supervisor

Asst. Prof. Abdullah DEMİR

by

Serdar ŞENGÜL

December 2023

©2023[Gaziantep University]

I hereby declare that all information in this document has been obtained and presented in accordance with academic rules and ethical conduct. I also declare that, as required by these rules and conduct, I have fully cited and referenced all material and results that are not original to this work.

Serdar ŞENGÜL

ABSTRACT

DESIGN AND FABRICATION OF HIGH-POWER LASER DIODE BAR

ŞENGÜL, Serdar
M.Sc. in Optic and Acoustic Engineering
Supervisor: Prof. Dr. Ahmet BİNGÜL
Co-Supervisor: Asst. Prof. Abdullah DEMİR

December 2023

66 pages

Semiconductor lasers have emerged as a transformative technology replacing conventional methods with their rapid evolution and widespread integration across various industries. It is increasing its impact in the industry involving material processing, tempering, annealing and bending. Laser diode bars are increasingly utilized in these processes, offering the advantage of easily adjusting the optical power and beam dimensions to meet specific requirements. This thesis as part of the TUBITAK-1004 project, investigates the details of laser diode bar fabrication for a system designed to execute heat treatment processes on glass surfaces. Utilizing high-power laser diode bars, the goal is to achieve optical power exceeding 100 W using 1-cm bars. The focus is to apply heat treatment by these bars to glass surfaces containing coatings with silver layers, a task traditionally implemented with large and energy-intensive furnaces. In contrast to traditional techniques, the use of laser diode bars provides precision targeted heating, considerably reducing energy usage and processing time. Heat distribution management in various glass treatments has the potential to transform the glass industry by adding flexibility to the relevant processes. This thesis demonstrates the fabrication of high-power laser diodes achieving an output power of 158 W, also showcases their practical application. The conducted heat treatments on coated glass surfaces are analyzed. The outcomes presented in this study demonstrate an outlook of the implementation of these laser diodes for industry.

Key Words: Laser Diode Bar, High Power Laser, Laser Heat Treatment

ÖZET

YÜKSEK GÜÇLÜ DİYOT LAZER BAR TASARIMI VE FABRİKASYONU

ŞENGÜL, Serdar
YüksekLisans Tezi, Optik ve Akustik Mühendisliği
Danışman: Prof. Dr. Ahmet BİNGÜL
İkinci Danışman: Dr. Abdullah DEMİR

Aralık 2023

66 sayfa

Yarı iletken lazerler, hızlı gelişimleri ve çeşitli endüstrilerdeki yaygın entegrasyonları ile geleneksel yöntemlerin yerini alan dönüştürücü bir teknoloji olarak ortaya çıkmıştır. Malzeme işleme, temperleme, tavlama ve bükme gibi fiziksel şekil değişikliklerini içeren endüstrideki etkisini artırmaktadır. Lazer diyot çubukları, bu işlemlerde giderek daha fazla kullanılmakta ve belirli gereksinimleri karşılamak için optik gücü ve ışın boyutlarını kolayca ayarlama avantajı sunmaktadır. TÜBİTAK-1004 projesinin bir parçası olan bu tez, cam yüzeylerde ısıl işlem süreçlerini yürütmek üzere tasarlanmış bir sistem için lazer diyot çubuğu üretiminin ayrıntılarını araştırmaktadır. Yüksek güçlü lazer diyot çubukları kullanılarak, 1 cm'lik çubuklarla 100 W'ı aşan optik güce ulaşılması hedeflenmektedir. Odak noktası, geleneksel olarak büyük ve enerji yoğun fırınlarla uygulanan bir görev olan gümüş katmanlı kaplamalar içeren cam yüzeylere bu çubuklarla ısıl işlem uygulamaktır. Geleneksel yöntemlerin aksine, lazer diyot çubuklarının entegrasyonu, tam olarak ihtiyaç duyulan yerlerde lokalize ısıtma sağlar, enerji tüketimini ve işlem süresini önemli ölçüde azaltır. Çeşitli cam işlemlerinde ısı dağılımının kontrolü, ilgili süreçlere esneklik kazandırabileceğinden cam endüstrisinde önemli etki yaratma potansiyeline sahiptir. Bu tez, 158 W çıkış gücüne ulaşan yüksek güçlü lazer diyotların üretimini göstermekle kalmıyor, aynı zamanda pratik uygulamalarını da sergiliyor. Kaplanmış cam yüzeyler üzerinde gerçekleştirilen ısıl işlemler analiz edilmiştir. Bu çalışmada sunulan sonuçlar, endüstriyel uygulamalar için bu lazer diyotların uygulanmasını göstermektedir.

Anahtar Kelimeler: Diyot Lazer Bar, Yüksek Güçlü Lazer, Lazer Isıl İşlem

''Dedicated to people who I lost in the earthquake on February 6, 2023''

ACKNOWLEDGEMENTS

I would like to thank my co-supervisor, Asst. Prof. Abdullah Demir for his guidance and support throughout the study. I am thankful for his encouragement and motivation. I would like to thank Prof. Dr. Ahmet Bingül for his support since my undergraduate education and for his support and convenience during my master's study. I am grateful for everything he contributed to me. I would also like to thank Dr. Babak Olyaeefar for his suggestions, evaluation of the thesis and invaluable feedback throughout the study.

I would like to thank all my companions, colleagues, and individuals of the Nanophotonic Devices Research Laboratory (NanoPhD Lab), Abdulmalik Abdulkadir Madigawa, Enes Şeker, Doğukan Apaydın, Turgay Bebek, Ali Kaan Sünnetçioğlu, Kaveh Ebadi, Ece Karabey, Osama Adil Saadi, Yasaman Salimi, and Eylül Badal for making my time valuable while working in ARL. It has been a pleasure to share numerous great recollections with you all. I would like to give special thanks to UNAM cleanroom staff Taha Ilıkkan. Murat Güre, Ergün Karaman, and Mustafa Özer for their support in the cleanroom.

Within the scope of this study, I would like to thank Burak Ünal for his support, Burak Okan from Şişecam for the characterization of coated glasses and their laser heat treatment, Enis Işık from Ermaksan for laser bar characterization and laser heat treatment tests, and finally Emre Ünal, one of the group members of UNAM director Hilmi Volkan Demir, for his contributions to the characterization of mirror coatings.

I would like to especially thank Betül Konaklı, Yusuf Satıcı, Onur Kalaycı, and Pelin Burgu for their valuable friendship and support in difficult times.

I wish to extend my gratitude to my mother Aycan Ebru Şengül, my father Mehmet Şengül, my sister Efsu Şengül, and my brother Mustafa Şengül for their endless love. Thank you for being here.

This work was financially supported by TUBITAK 1004 project (20AG024).

TABLE OF CONTENTS

Page

LIST OF TABLES

LIST OF FIGURES

Page*

LIST OF SYMBOLS

μ Micron

LIST OF ABBREVIATIONS

ARL	Advanced Research Laboratory
FAC	Fast Axis Collimator
HR	High Reflectivity
AR	Anti-reflectivity
PR	Photoresist
PECVD	Plasma Enhanced Chemical Vapor Deposition
RTP	Rapid Thermal Processing
COBD	Catastrophic Optical Bulk Damage
COMD	Catastrophic Optical Mirror Damage
CW	Continuous Wave
QCW	Quasi-Continuous Wave
LIV	Light Power – Current – Voltage

CHAPTER 1
INTRODUCTION

1.1 Motivation of Study

In this research project under the TUBITAK-1004 initiative, the conventional use of furnaces or fiber lasers in industrial heat treatment processes for materials like glass is being replaced. By utilizing high-power diode laser bars, the goal is to enhance the light intensity for more effective heat treatment on the target material. Upon the successful conclusion of the relevant investigations, the objective is to implement heat treatment processes on glass surfaces using these advanced laser technologies.

The use of fiber lasers in current studies has increased the interest in this field due to the intensity of the beam and the fact that it is around 100 µm. Losses in the coupling of the laser to the fiber reduce the efficiency to around 30%. This efficiency is an optical parameter that shows how much light power is obtained from the current and voltage applied to the laser. Since the use of high-power laser bars with low losses instead of these will contribute to increasing the efficiency to around 70%, the requirements can be achieved by using high-power diode laser bars with a lens that will provide collimation in front of them in such heat treatment applications.

As a result of obtaining 1-cm bars by fabricating 24 single lasers side by side and providing a minimum of 100 W optical power from these lasers, it is aimed to perform this process by heat treatment of the glasses, including the silver layer, which was previously produced by Şişecam. The idea of applying this heat treatment during production by placing the full bars side by side and placing them on the bands in the glass production line, the details of the production and characterization of the laser bars to be used in this study, which is unique in our country with the project to be produced locally with the TÜBİTAK-1004 project, has been the motivation source of this study.

To realize the heat treatment process of the bars produced, they need to be professionally industrial packaged. In this context, after the design of the epitaxial structure was realized and this design was produced abroad, all fabrication processes were carried out in the clean room and the packaging process was transferred to the project partners again for packaging and this packaging process was carried out.

In this context, the lasers were first cleaved and each bar was separated from each other. The bars, whose facets are cleaved, are coated with SiO_2 and TiO_2 dielectric mirror coatings in pairs in the device where these coatings will be made by using the appropriate adapters for mirror coating.

One facet of these lasers, which radiate from two facets, is made to have high reflectivity while the other is coated with a single layer of coating to ensure that all the radiation reflected from the mirrors comes out of only one facet. At the same time, this single-layer coating protects the surface and ensures that the radiation emitted uniformly.

After all these processes, the laser bars are packaged according to the test setup and made ready for testing.

1.2 Laser

Readers of H. G. Wells's novel The War of the Worlds might conclude that the first laser device to be operated on Earth was brought here by Martian invaders a century ago, at least according to the description that;

“In some way, they (the Martians) are able to generate an intense heat in a chamber of practically absolute non-conductivity... This intense heat they project in a parallel beam against any object they choose, by means of a polished parabolic mirror of unknown composition... However itis done, it is certain that a beam of heat is the essence of the matter. What is combustible flashes into flame at its touch, lead runs like water, it softens iron, cracks and melts glass, and when it falls upon water, that explodes into steam." (From Pearson’s Magazine, 1897.)[1].

After this interesting and yet fantastic definition of laser, if we need to make a more theoretical definition, lasers, also known as "Light Amplification by Stimulated Emission of Radiation," are incredibly strong and adaptable tools that have revolutionized a wide range of industries as well as the realms of science, technology, health, and business [2],[3].Since its early conception in the middle of the 20th century and the widespread use of lasers today, they have been used for a broad range of purposes, from scientific research to common consumer goods.

When Albert Einstein put out the hypothesis of stimulated emission in 1917, the first lasers were thought to exist. The first functional laser, the ruby laser, was created by Theodore H. Maiman, not until the 1950s [1]. This discovery opened the door for more investigation and development, which resulted in the creation of several kinds of lasers, including semiconductors, gas, and solid-state lasers. Laser technology has significantly improved, allowing for an ever-growing number of applications.

The fundamental principles behind lasers, their historical development, and their significant impact on various disciplines are explored in this chapter by the details.

Lasers use a technique known as stimulated emission to produce coherent light [4].In this process, photons interact with atoms or molecules in the medium to release new photons that are in phase with the incident photons and have the same wavelength and direction. This coherence makes it possible to narrowly concentrate laser light into a beam with a high intensity and low divergence [4].

Lasing is the consequence of a chain of appropriate circumstances. A pump source to excite the electrons, an active material with a higher refractive index than the surroundings, and a feedback mechanism appropriate for the emission wavelength make up a laser [5].The lasing process begins with absorption due to the presence of these components. The pump source then stimulates the gain medium's atoms, causing electrons to migrate into the excited states. When there are more excited state electrons than ground state electrons, a population inversion occurs. After population inversion, electrons fill the excited state and emit a photon to return to the ground state. It is known as spontaneous emission. When the excited electrons are brought down to the ground state, an identical photon with the same frequency and phase is produced. This photon interacts with the other excited electrons. Stimulated emission is the process wherein the quantity of photons doubles with each contact.

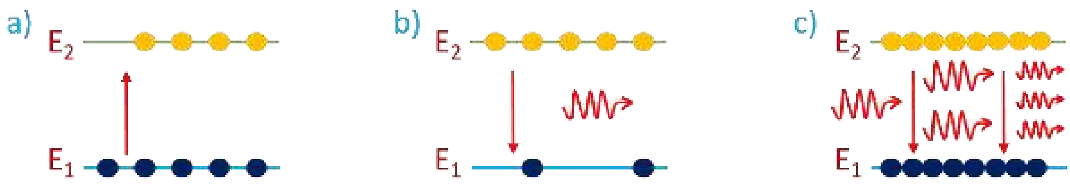

Figure 1-1. a) Absorption b) Spontaneous Emission c) Stimulated Emission.

Absorption; the gain medium absorbs the energy from the pump, causing electrons to be stimulated from their ground states. Spontaneous emission, as the excited electrons go back to a lower energy state, they spontaneously emit a photon to release their stored energy. Stimulated emission is electronic transitions are made possible by stimulating electrons with a photon rather than allowing them to freely decrease to a lower state [5].

When talking about lasers, it was mentioned that there are three basic elements: source, cavity, and gain mechanisms. Under the title of source, absorption, spontaneous emission, and stimulated emission were mentioned in detail. As for the cavity, it is theoretically known that lasers are cleaved, their facets are mirror-coated, and the light is emitted from the facets.[6] Figure 1-2 a shows the simulation result for the refractive index profile of the epitaxial structure and the vertical near-field profile used in the thesis. The laser diodes aim to achieve high output power combined with high power conversion efficiency (PCE) above 60% to provide cost-effective laser modules.[7-9] [10]

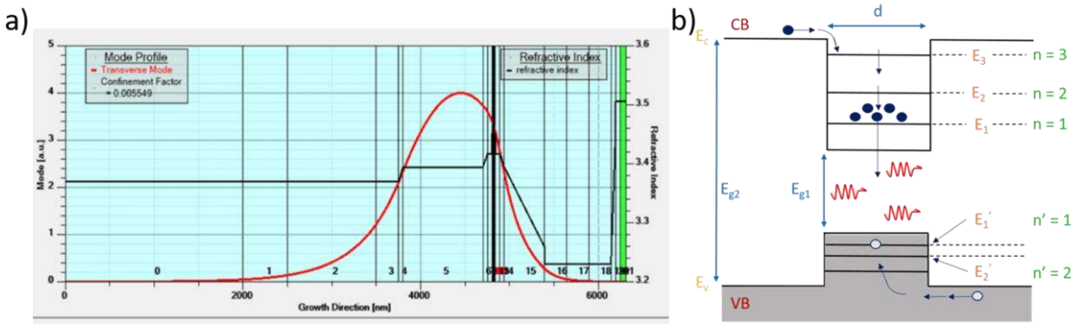

Figure 1-2. a) Simulation results for the refractive index profile of the epitaxial structure and the vertical near field profile. b) Electron-hole pair recombination and stimulated emission mechanism.

1.3 Edge-Emitting Laser Diode

As the name implies, edge-emitting laser diodes emit light from their facets-like mirrored surfaces [11]. When a laser diode has been switched on, some of the laser light passes through one facet of the active layer and transforms into a laser beam that is emitted. The beam at the emission facet is a little larger than the cross-section of the active layer of a laser diode and has an elliptical shape because the active layer of a laser diode has a rectangular-shaped cross section and some of the laser fields will leak out from the active layer due to the limited confinement [1].

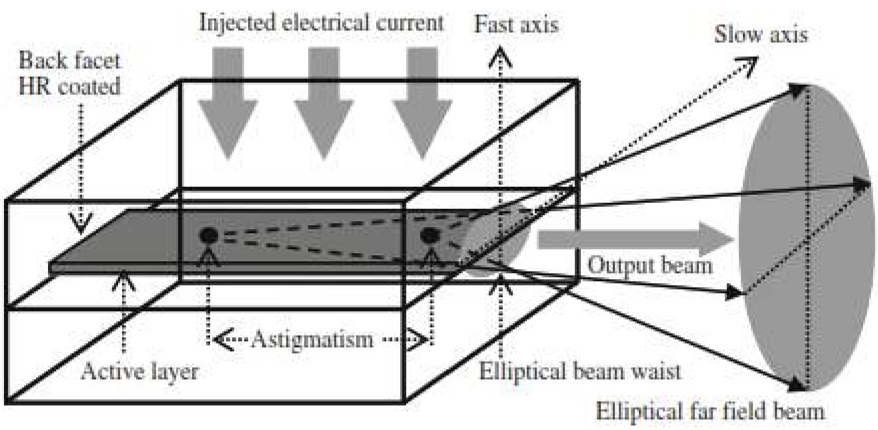

Figure 1-3. Edge emitting laser structure and emission regions[4].

As seen in Fig. 2, the semiconductor gain region inside the structure produces photon, by carrier recombination in the quantum well, and the optical waveguide guides the light to the coated facet. A semiconductor laser's vertical and lateral axis called fast- and slow-axis, respectively, due to their divergence features. The rear facets have a highly reflective (HR) mirror that allows them to benefit from the gain medium when light is reflected by the mirrors. This is the rationale why the rear facet is covered with a highly reflective (HR) material. At the same time, the front facet gains the anti-reflecting (AR) for the light beams coming from the gain medium. By courtesy of coating, the laser light is collected from one facet. The following chapter will go into detail on HR and AR coating materials [11].

However, the HR and AR coated facet came about by a cleaving procedure. The cavity length is controlled by the special diamond tool from the top surfaces of the laser scratched manually. Afterward, cleave the lasers together by bending them with an equal amount of force. All the crystals in the wafer structure are cleaved from each other along the way to create facets perpendicularly and horizontally.

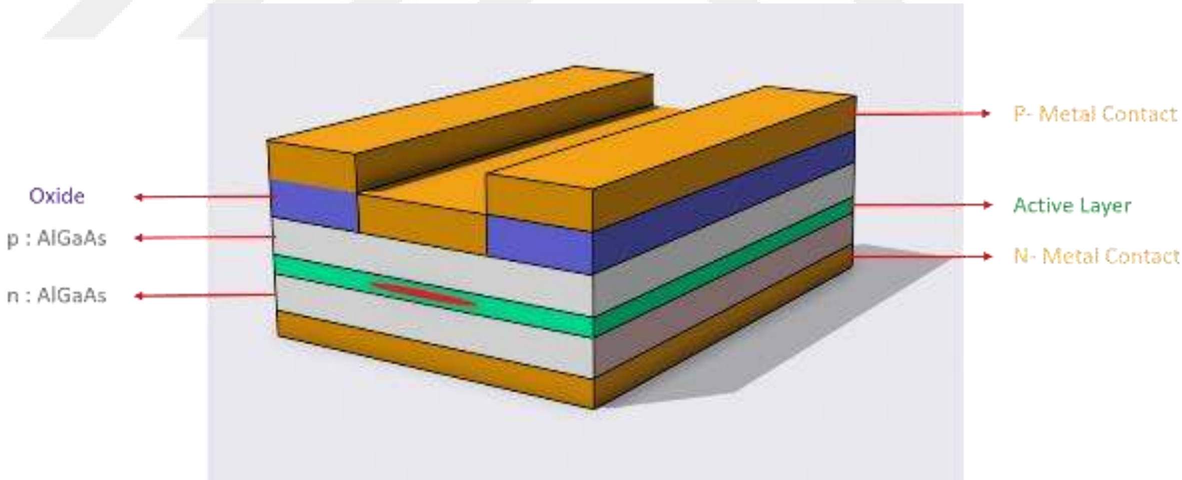

Figure 1-4. Cross-sectional diagrams of a semiconductor laser diode looking in the sideways direction.

In light of this information, our laser diode structure is schematized above along the lateral direction. The top and bottom surfaces are coated with gold to create a contact on this chip structure. Oxide layers prevent the current injection from the undesired regions. The top and bottom surface of the active layer has doped GaAs layers p and n types to create electron-hole pair in our laser diode structures.

1.4 High-Power Laser Diode

Due to their small size, high efficiency, and adaptability, semiconductor laser diodes have revolutionized many areas of technology and research [4], [11]. High-power semiconductor laser diodes that can generate high optical power while preserving semiconductor lasers' primary advantages have become increasingly popular in recent years [12]. As a result, high-power semiconductor laser diodes have developed significantly, creating new opportunities in industries including telecommunications, industrial applications, military systems, and medical equipment [13].

A semiconductor laser diode is a device that uses stimulated emission to transform electrical energy into coherent light[4]. Semiconductor lasers, as opposed to gas or solid-state lasers, rely on the characteristics of semiconductors, which are often made of composite materials like gallium arsenide (GaAs) or indium phosphide (InP) [5]. These materials are selected because of their distinctive electrical characteristics, which enable effective light emission when a current is applied.

A high-power semiconductor laser diode's basic construction is made up of numerous essential elements [14].The active area, sometimes referred to as the gain region, is the laser diode's heart and is where light is produced. It generally consists of a number of quantum dot or well layers, which keep electrons and holes in a small space and promote effective recombination and light emission [4].

Semiconductor laser diodes require a method of efficient heat dissipation in order to operate at high power levels [15]. Overheating during operation can cause irreversible damage and performance decline [16]. The utilization of heat sinks, thermoelectric coolers, and micro-channel cooling systems are just a few of the several heat management strategies that are used. By maintaining ideal operating temperatures, these methods guarantee the stability and dependability of high-power semiconductor laser diodes [11], [17].

The emergence of optical phenomena such as optical loss, thermal effects, and nonlinearities is one of the major difficulties in the development of high-power semiconductor laser diodes [5].The output power and efficiency of the lasers may be constrained by these phenomena. Ingenious designs and cutting-edge materials have been used by scientists and engineers to minimize these problems, leading to notable advancements in power scaling and overall performance [11].

The power levels of high-power semiconductor laser diodes which generally range from several watts to many kilowatts are used to categorize them [18],[13]. They have numerous uses in many fields. High-speed laser diodes are used in telecommunications to transmit data with reliability across long distances using optical fiber networks [19]. Additionally, they play a crucial role in high-resolution laser printing and laser projection systems, which produce vivid and clear pictures [20].

High-power semiconductor laser diodes are used in industrial settings for operations including cutting, welding, and material processing [20],[21]. They are perfect for production operations that need accuracy and efficiency because of the precise control and high output [14],[22]. Additionally, they are used in defense systems like target identification and laser-guided missiles, where their dependability and compactness are crucial [21].

High-power semiconductor laser diodes have use in the medical industry as well, notably in laser surgery and therapeutic uses [19]. Surgeons can carry out delicate treatments with the least amount of invasiveness thanks to their capacity to provide regulated and accurate laser beams. In dermatology, laser diodes are also utilized for a variety of procedures, such as tattoo removal, skin resurfacing, and hair removal [20].

High-power semiconductor laser diodes have become essential components in a variety of applications, to sum up. They are now vital in telecommunications, industrial operations, defense systems, and medical procedures because of their small size, great efficiency, and versatility. High-power semiconductor laser technology is constantly evolving as a result of ongoing research and development projects that push the limits of performance and power scalability [23],[24].

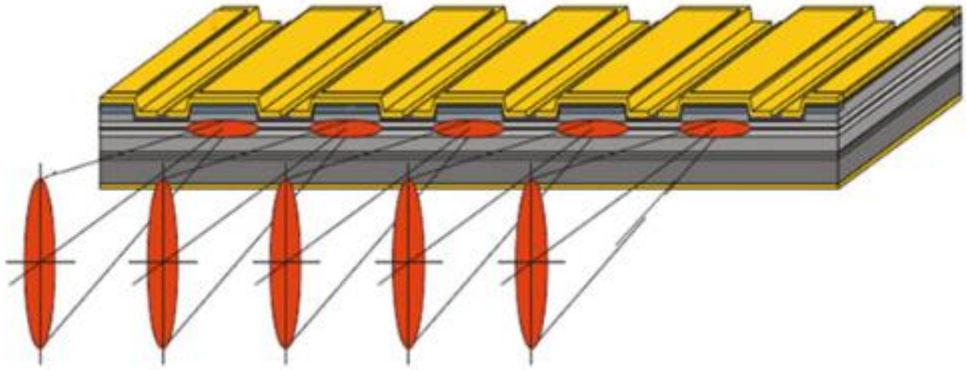

Figure 1-5. Edge emitting bar laser structures active emission region from quantum wells[11].

Figure 1-5 shows a high-power laser diode bar's schematic view. Due to the power, heat, and current injection area limits of each laser, many single laser waveguides are gathered together in a single device which is called as laser bar in the industry [25].

1.5 Outline of the thesis

The first chapter provides an extensive summary, covering fundamental ideas and a brief history of lasers. This chapter begins with an explanation of the working principle and basic mechanics of edge-emitting lasers and then continues on to a brief overview of the dynamics of edge-emitting lasers. The chapter finishes with a summary and general information regarding high-power laser diodes, which are the motivation for this thesis.

The second chapter deeply discusses the manufacture of high-power laser diodes, which is the motivation of this thesis. This chapter describes the production of the single emitter and the manufacture of the bars, beginning with the mask design step. The last section of this chapter summarizes information regarding the mirror coating process of the associated lasers.

Chapter 3 contains details of the process related to the packaging of laser bars. Afterward, information about the test setup designed and installed for the testing and characterization of the lasers is shared.

Chapter 4, where the test and characterization results of the fabricated laser bars are shared, is the section where the data obtained are presented.

Chapter 5 is the section where the laser thermal process application, in which lasers that meet the requirements will be used, is discussed and information about this process is shared.

CHAPTER 2
FABRICATION OF HIGH-POWER LASER DIODES

The manufacturing of a laser diode should be realized in the clean room. The device that we deal with should be produced in a special environment different from the normal laboratory conditions. These kinds of devices need to be placed where cleaned, temperature controlled, sometimes vacuumed, and in special atmospheric conditions for high efficiency and long-term lifetime. During their fabrication special devices are also used to produce them which is appropriate for the clean room. Particularly delicate and sensitive sections are the facets of the laser diode. The laser emission facet is critical for the functionality of the device because [26],[27].

2.1 Mask Layout

The optical lithography mask layout should be carefully planned by the researcher, who should then test it several times by stacking all of the mask layers to determine if the patterns line up as intended. Designing an optical lithography mask is the first step in the production of a device. The generated design was printed on the quartz glass by the Cr layer with the help of a mask-writer machine, which is frequently used in optical lithography.

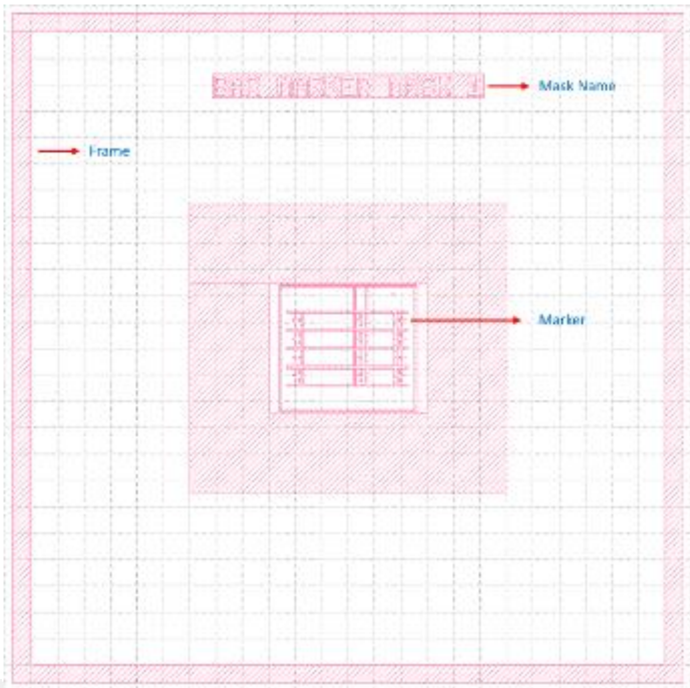

Figure 2-1. Schematic view of mask design

A "dark field mask" and a "clear field mask" are both used in optical lithography. If there are more open spaces than confined spaces, it is referred to as a "clear field mask". A "dark field mask" is one that has more Cr components than other parts. When aligning the sample to the mask during optical lithography and utilizing a dark field mask, it will be difficult to detect your sample using a camera because all you can see is the mask. To address this issue, we added a frame to each step that makes it simple to locate and do the rough alignment. To do rough alignment, outline frame used while alignment process on the sample. As an illustration, you can see the frame and the marks on a clear field mask in Figure 2.1. This frame may not appear to be important at first glance, but it really makes alignment quite simple, especially if you're using a dark field mask. The sample alignment is the most difficult part of optical lithography. You must spend more time developing markers for precise alignment if your mask aligner is a manual device with a camera. This project involves seven lithography stages, which entails six alignments for the manufacturing of a single device. The left and right side of the chip were marked with four starting markers on each side of the chip in the first phase for the second mask alignment, as illustrated in Figure 2.2. We placed a marker to correspond with the first marker in the subsequent phase.

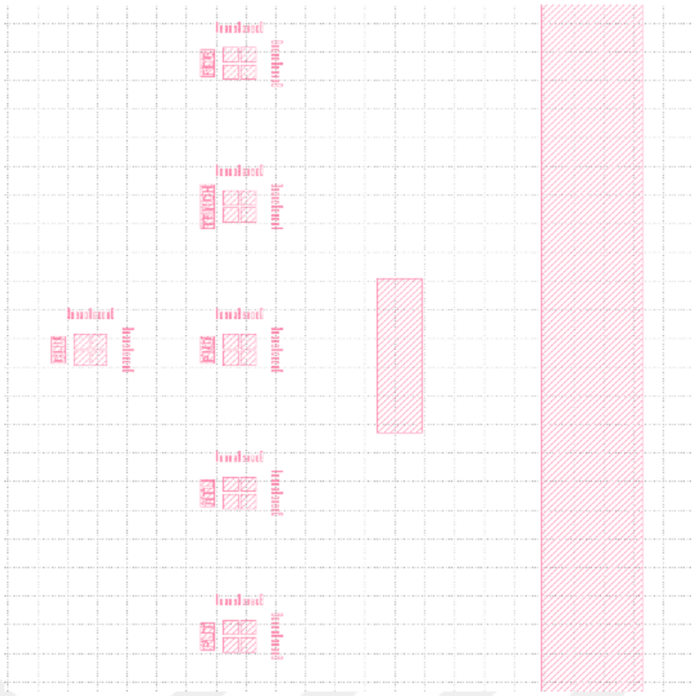

Figure 2-2. Markers of the mask

The markers schematized in Figure 2.2 are the guides to be used in all operations of the respective process. All markers lithographed with the first mask will guide the alignment of subsequent processes. With these alignment markers, which are frequently used in the industry, alignment can be done with an accuracy of 1 µm.

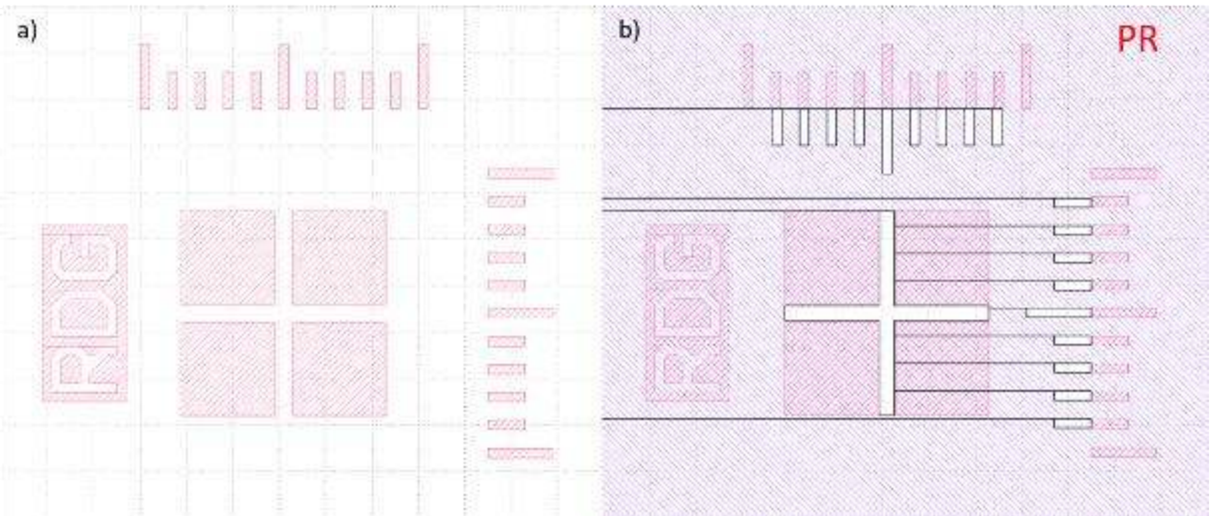

Figure 2-3.a) Marker alignment view with masks b) The image of the sample which PR coated on the sample and the mask aligned

All guide alignment marks are lithographed using the first mask in Figure 2.3. a. Then, using the marker of the appropriate procedure, alignment is carried out on all masks that will overlap these masks. After the first mask is printed (see Figure 2.3. a), photoresist is evenly applied with a thickness of about 500 nm to the whole surface of the laser sample.

The second mask, the ridge mask, is applied to the sample using the mask aligner device, aligned with the matching micro-manipulator using the aligner markers, and then subjected to UV light. The photoresist chemical layer that was applied to the sample has its structure broken on the surfaces of the corresponding laser structures, such as the crosshair in the middle of the aligner marker. The required structure is then created after it has been chemically decomposed using another chemical developer.

2.2 Single Emitter Fabrication

Device manufacturing should apply cautiously to realize a reliable fabrication. The recipe that is used for fabrication has been prepared in detail. A total of 6 major processes and more than 450 steps are involved in putting the chip developed into the device package. We have used our facilities to fabricate high-power laser devices according to the fabrication technique shown below as clearly as possible.

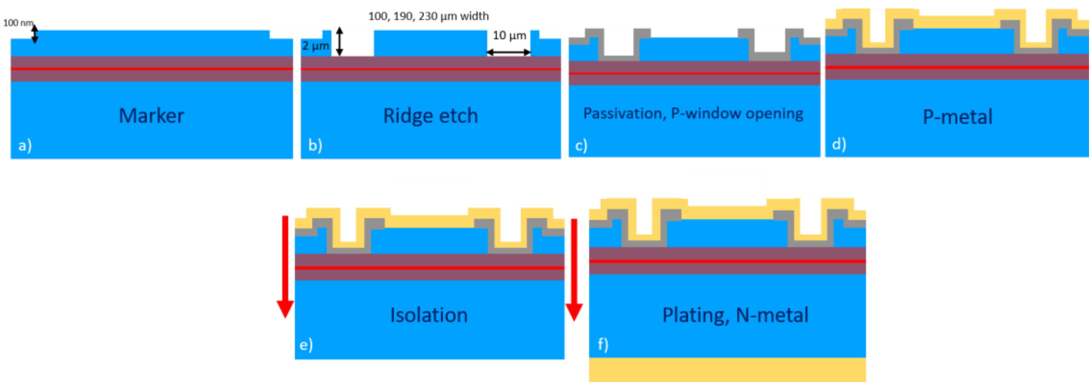

Figure 2-4. Single Emitter High-Power Laser fabrication steps (a-f)

To define shape and property, each major process requires detailed information. An optical microscope image is demonstrated for the method mentioned above in figure 2.5.

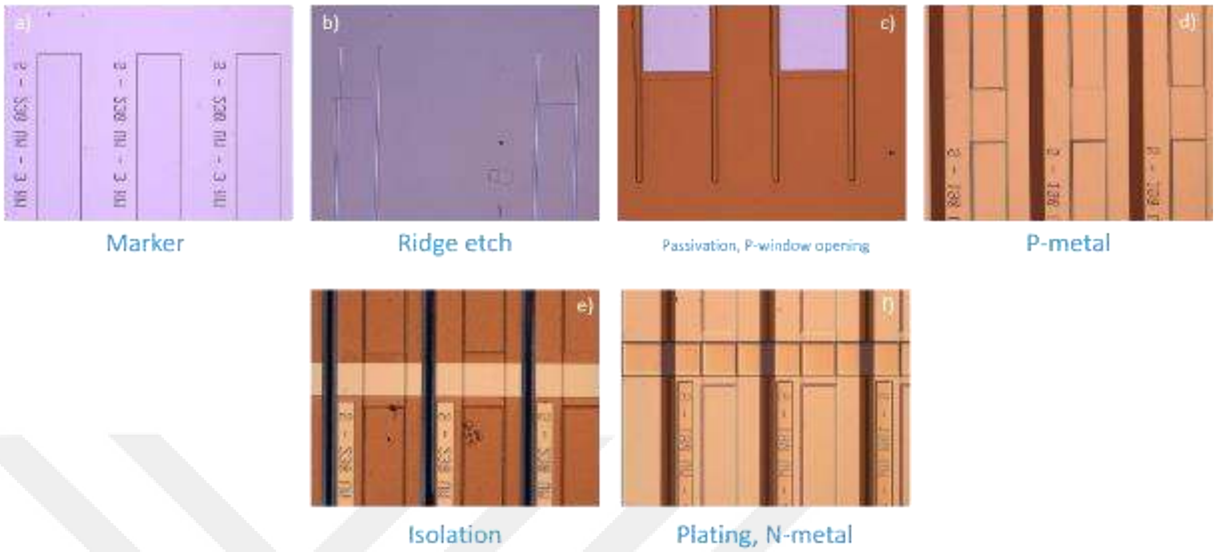

Figure 2-5. Single Emitter High-Power Laser fabrication steps (a-f) optical microscope images

To avoid duplication, every significant step in the manufacture of bars will be explained in detail. Following the mask manufacturing, the fabrication was done several times to ensure that the mask and process steps are appropriate. For the single emitter fabrication, we fabricated waveguides with various lengths of 3, 4, and 5 mm and different widths of 100, 190, and 230 μm. According to the test conclusion, the best and optimum waveguide width and length are chosen. This test can be used to to characterize the internal loss and internal quantum efficiency of the chips.

2.3 Bar Fabrication

To begin production on the GaAs laser wafer that we have designed, we cleave a sample whose dimension is defined by the mask's dark and light frames. On a single full wafer, around 9 separate fabrications of a variety may be made. The surface must be immaculate and devoid of scratches after cleaving. The 2.5 cm X 2.5 cm sample is cleaved through GaAs, as shown in Figure 2.6. The sample is cleaned with acetone, alcohol, and water after cleaving. A quick descum will keep undesired dirt and stains from building up on the sample surface in the future, preventing lasting stains and smudges. Following this quick cleaning step, fabrication may start.

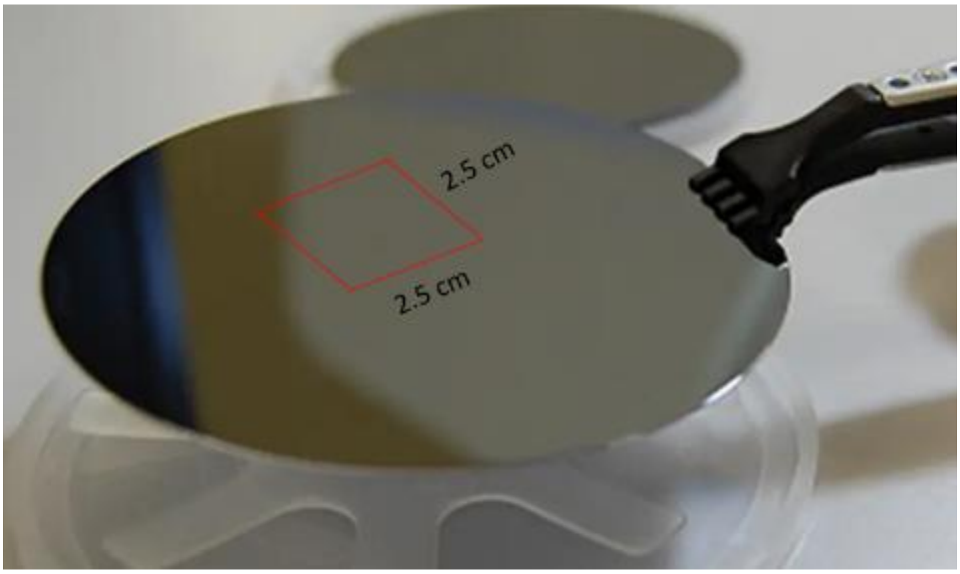

Figure 2-6. GaAs wafer cleaving for the fabrication start

Marker Layer Etch

For the marker stage, the photoresist is first coated all over the sample. Then the marker mask is aligned on the sample with the mask aligner. After the alignment process is performed so that the margins are equal for each edge, the exposure process is performed. While the places under the dark parts of the mask are not exposed to the exposure process, the remaining places are exposed to this exposure, and the structure is chemically disrupted. After the exposure process, the pre-optimized time is developed with a longitudinal developer solution. Open areas exposed to exposure are purified from photoresist with this solution. We remove the cover layer by chemical etching. To do this, diluted phosphoric acid and hydrogen peroxide are used. In this solution, hydrogen peroxide oxidizes the surface, and in about 40 seconds, phosphoric acid etching the highly doped 100 nm GaAs layer. At the end of process, in the epitaxial design, we have a 250 nm-thick, highly doped GaAs (Gallium Arsenide) cap layer. The laser cavity length etching close to the facet areas is also defined.

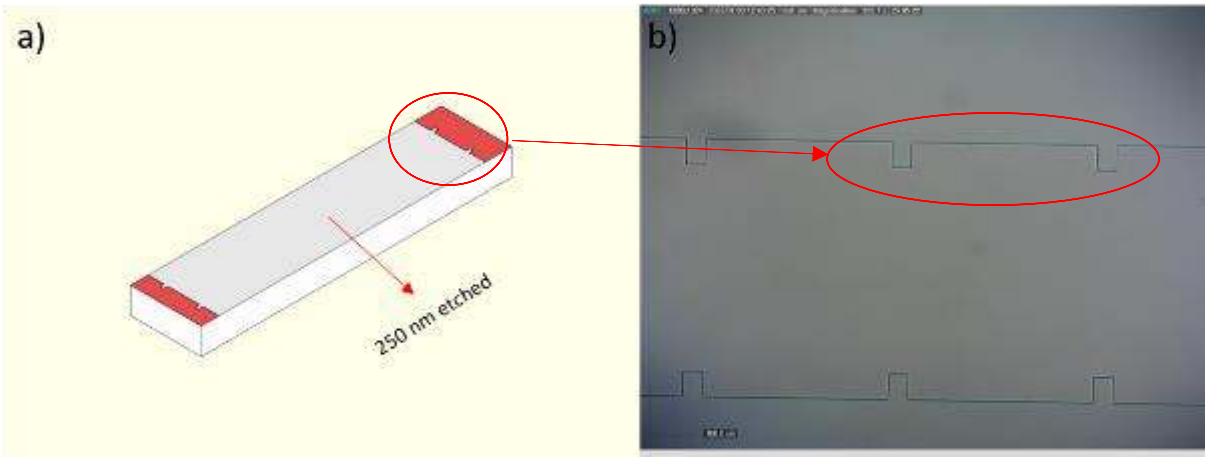

Figure 2-7. a) Schematic view of marker layer from top b) After the marker layer had been removed, the device's top was photographed using a 5x optical microscope.

The ridge, where the waveguides will be located, is positioned on these etched areas. The marker layer of the laser structure has been obtained and the contact layer has been removed where the current is not to be transmitted. The silicon nitride layer adheres better to rough surfaces created by chemical etching everywhere. As an electrical isolation layer, silicon nitride is used to prevent electricity from entering the waveguide. By shielding the facet from current leakage, cap layer etching further lessens the likelihood of catastrophic optical mirror damage.

Ridge Etch

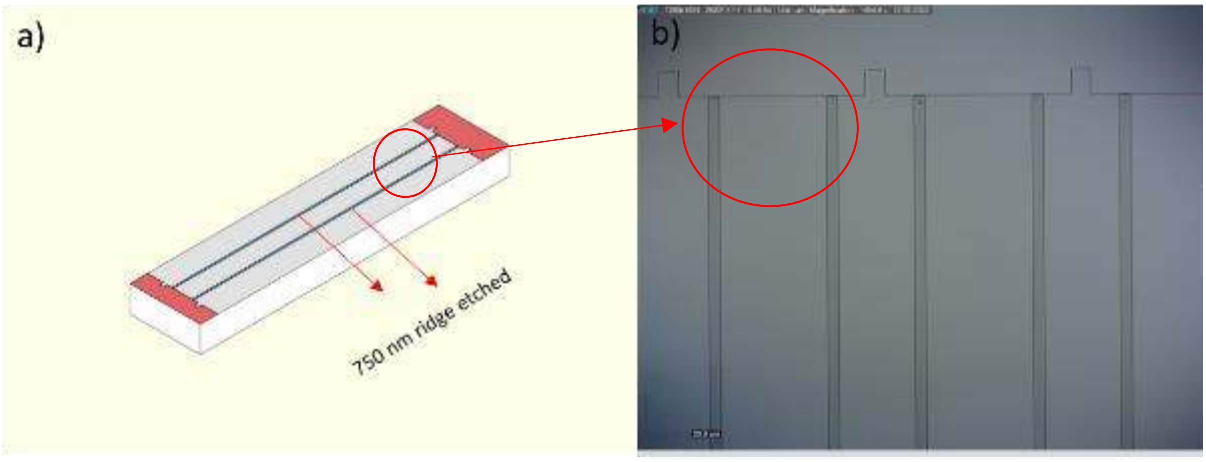

Figure 2-8. a) Schematic view of ridge structure from top b) After the ridge had been removed, the device's top was photographed using a 5x optical microscope

The process for determining the area where the current will be transmitted by touching the top surface of the laser is shown in the waveguide image. After the alignment performed in the previous step, the exposure with the aligner device, the etch steps with the diluted chemicals detailed in the marker step after etching the exposed areas with developer were also used to create the ridge structures. With the solution obtained by mixing diluted phosphoric acid and hydrogen peroxide chemicals, 750 nm deep ridge cavities were formed in approximately two minutes and 30 seconds. Thanks to that step, we define the ridges that provide the refractive index difference for optical mode confinement in the corresponding ridge etch process.

Trench Etch

The sample is subjected to routine cleaning steps after each step. Photoresist residues outside the etch areas are cleaned with acetone and remover chemicals where necessary. Depending on the amount of pits opened, more effective cleaning chemicals are also needed. These steps are carried out to penetrate the corner edges of the pits more effectively and to clean the sample completely.

In this step, approximately 2 μm deep pits are created. These pits ensure that the 24 adjacent lasers on the full bar and the 12 laser structures on the half bar are isolated and separated from each other. They serve to separate the lasers from each other by being located between the small combs structures opened in the marker step.

Apart from the waveguides, shield etching, which is another etching process aimed at separating the lasers from each other by etching down 2 μm within the contact etching limits, is also shown in this image.

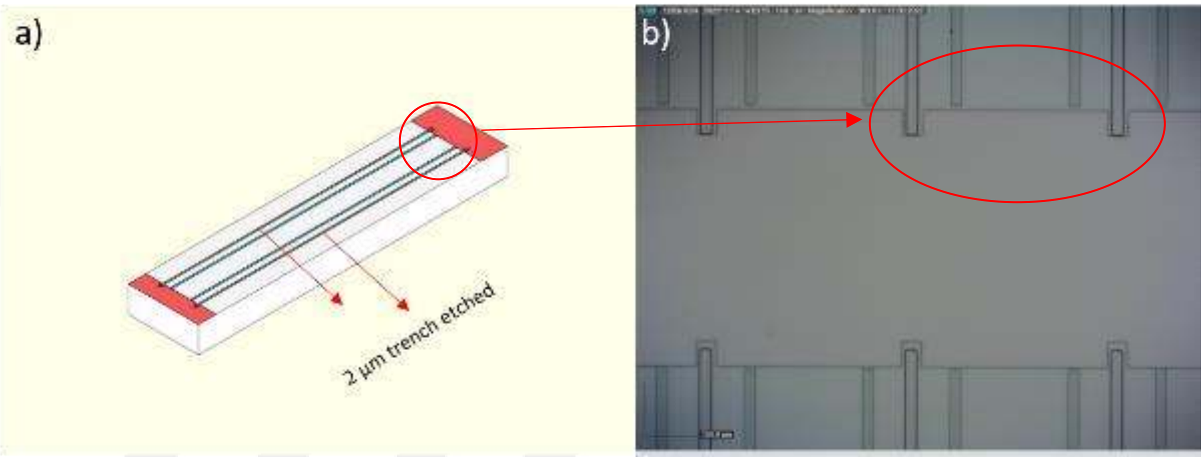

Figure 2-9. a) Schematic view of trench valley from top b) After the trench had been removed, the device's top was photographed using a 5x optical microscope

Cleave Etch

The bar constructions were said to have been created by positioning the individual 12 and 24 lasers on the half- and full-bars side by side as specified in the previous phase. The separation between these lasers is accomplished by cleaving a 2.5 cm X 2.5 cm sample. In order to make the cleave phase easier, the lithography process is employed, and pits are opened in certain locations much like in the previous steps. With this phase, the depth of these areas is increased and the width of these pits is modified in accordance with the diamond tips to be utilized for the cleave process.

The diamond bit will be used to drill tiny trenches around 5 μm deep to separate the half and full bars from one another. These cracked surfaces act as reflectors and exit surfaces for laser beams at the same time. Due to the need for extreme caution throughout the cleave process, it's critical to align the lithography accurately and open the appropriate pits uniformly and smoothly.

The sample is agitated in this manner with the same solution for around 10 minutes until a region of about 5 µm is pitted.

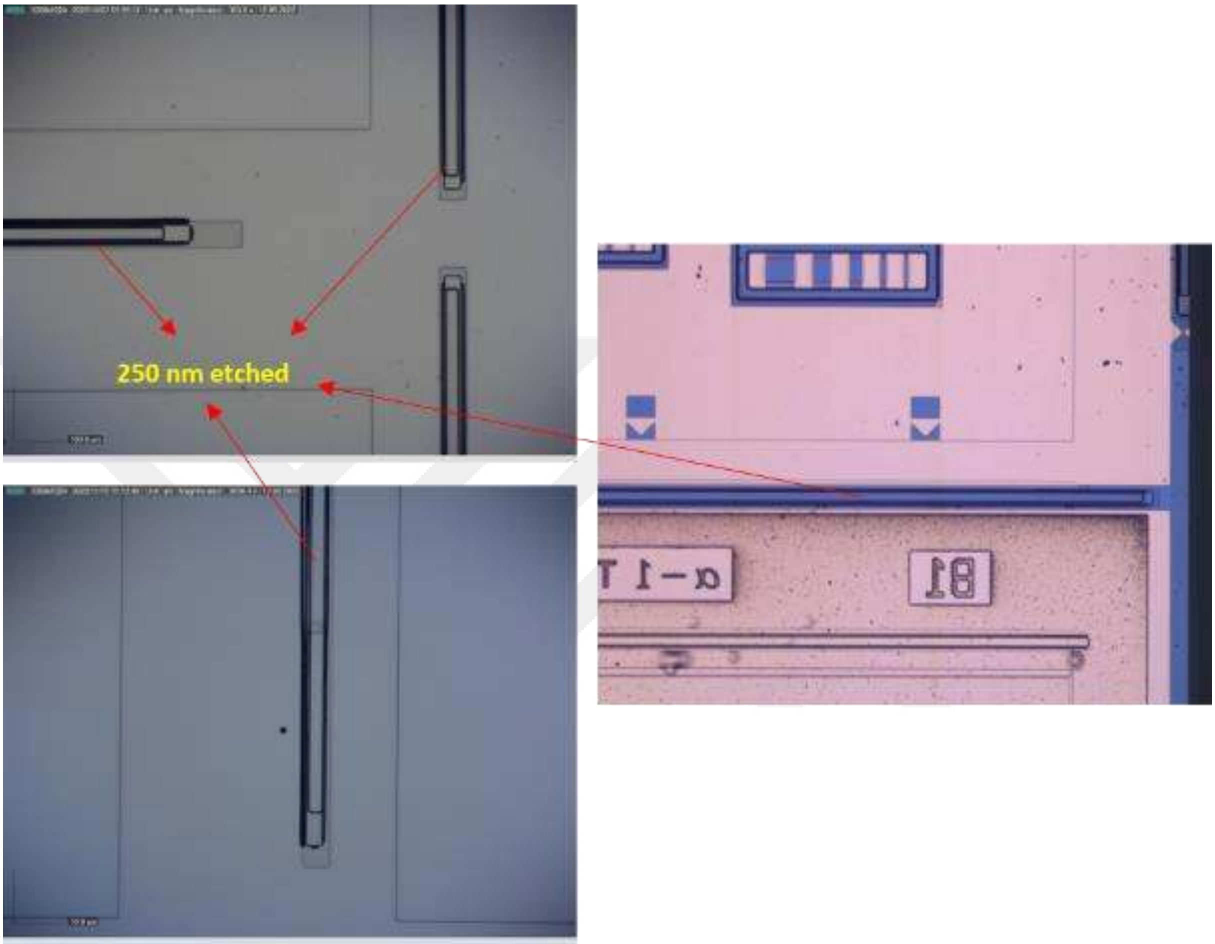

Figure 2-10. Schematic view of cleave valley from top

Dielectric Coating

Using PECVD (Plasma Enhanced Chemical Vapor Deposition), silicon nitride is coated on the sample's entire surface in this step. This coating process is used to identify the location where a laser's surface will be completely covered in dielectric material to prevent current transmission. In this situation, a coating is applied with a wavelength range of 100 to 150 nm.

The photoresist is completely covered before the lithography step begins. For the P-window, or the transmission of the current downstream from the structure and photon creation, the photoresist is produced in the necessary region. In this method, the waveguide structures will only retain their dielectric coating, while the other areas and the dielectric material at the bottom will still have photoresist on them. The following stage involves using BOE chemical to erode the residual SiN, the dielectric material, in order to make the current conduct without the use of any insulating layer.

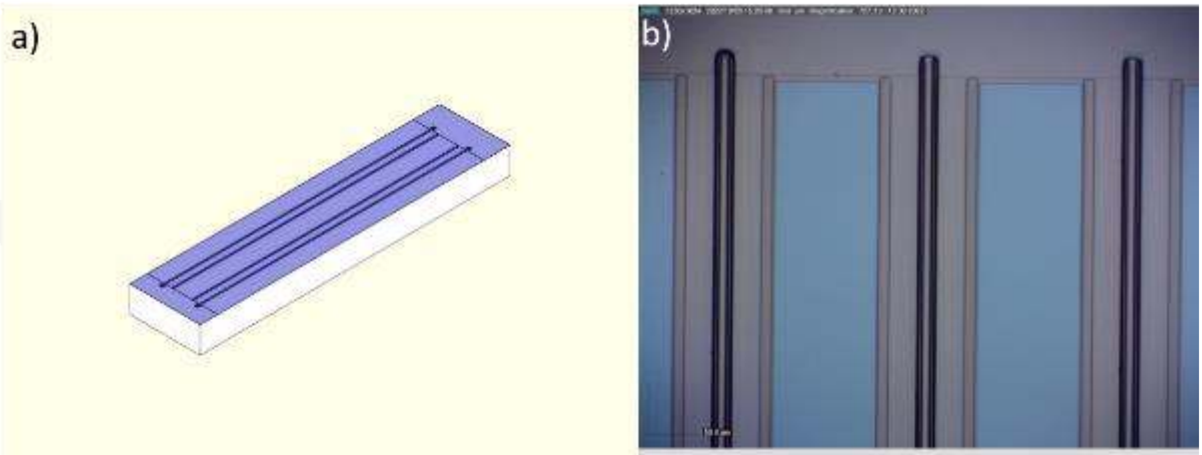

Figure 2-11. a) Schematic view of SiN coating from the top b) After developed of PR have been removed from P-window parts

P-Window Opening

P-window opening is the process that is used to establish the shape of the area where all photon production will occur. At this point, the waveguide's residual nitrate coating is cleaned with BOE abrasive, and the locations where the current will be transferred are entirely identified. The laser structure will now be able to emit light in this manner. Wherever current transmission is not required, the remaining areas will be blocked by the insulating dielectric substance. It will serve as a barrier against the current and have a significant impact on the width of the waveguide the laser emits. Thus, half and full bar laser structures with a width of 190 m will be capable of current transmission.

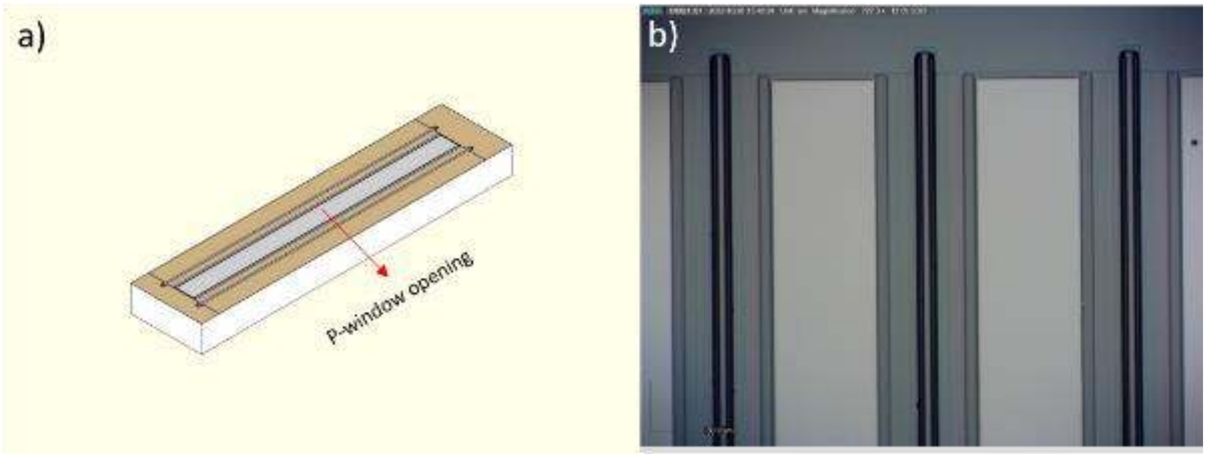

Figure 2-12. Schematic view of P-window opening from top, b) After BOE etched, SiN have been removed from waveguide's and pictured by optical microscope in 5X magnification

P Metal

The diode used in semiconductor lasers only permits current to travel in one direction. Metal layers and subsequent wire bonding are required for electrical pumping. Using a high current carrying tiny tip probe to allow homogeneous current to flow through to the laser is another method of driving semiconductor lasers. We lay down two metal layers as top and bottom contacts (p and n, respectively).

Because gold (Au) has a high conductivity, we deposit it. The issue with the gold is that it doesn't immediately attach to the GaAs surface. We begin deposition with 20 nm Ti (Titanium) via an e-beam evaporator because our substrate is GaAs. GaAs are attached to the titanium layer, which is adhered to by the other metal layers. To prevent gold diffusion during the annealing process, the Pt (Platinum) layer (40 nm) is continued to be deposited using an e-beam evaporation technique. Finally, we use e-beam evaporation to deposit a 100 nm gold coating. The ensuing lift-off procedure is made feasible by the e-beam evaporation's directed coating.

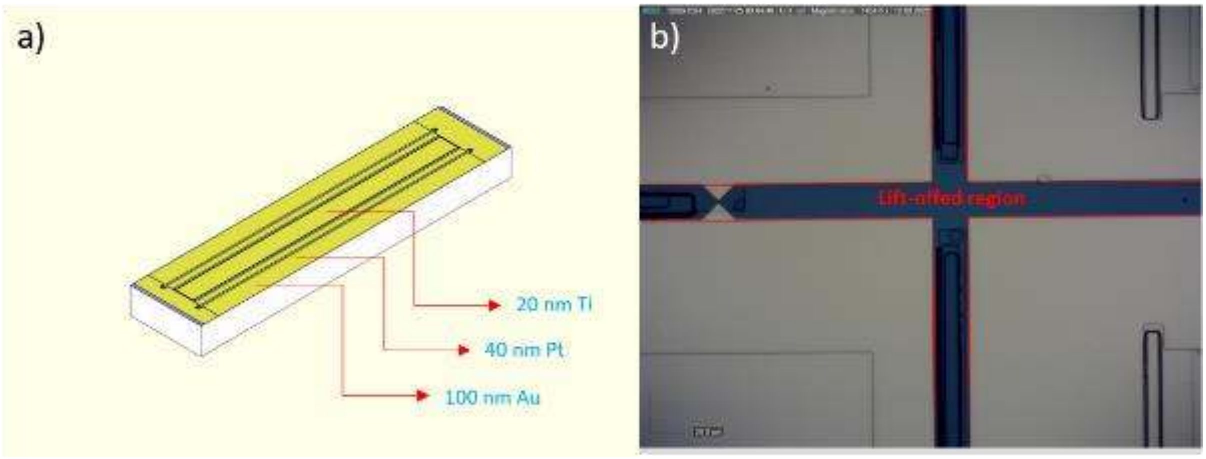

Figure 2-13. a) The top view of the laser with 20 nm Ti, 40 nm PT, and 100 nm gold plating is shown in the illustration, b) the lift-off areas of the metal coating, or the locations where the lasers are separated from one another, are shown in photos that were obtain

Titanium, platinum, and gold coatings have been applied to all laser surfaces, as shown in Figure 2.13 above, and these metals allow for the acquisition of the p-contact feature. Since there are bar structures, unlike single lasers, 12 and 24 laser structures in half and full bars lined up side by side have metals covering all of their surfaces. The metals in the juxtaposed regions must be removed in the cleave process in order to separate these laser constructions from one another. Due to the requirement to separate the lasers and offer the facets mirror characteristics, this procedure is crucial. Another benefit that will help the laser's cleave process will come from the lifting-off of the metals in these regions. Because there is a drawback that will prohibit the substrate from bending during fracture due to the restricted and shallow depth of these shallow holes containing metal.

One of the strongest signs that this stage was successful is the good lift-off process. The photoresist in the lift-off zones must first be effectively eliminated. This can only be accomplished by paying close attention to the temperature and time limits of the hard bake period, or the heating process, which is used to fully attach the initially applied photoresist. The E-beam device's anticipated vacuum level of 10e-6 millibars is another issue that must be taken into consideration in order to efficiently complete this step, which entails removing metals from the areas where the lasers must be separated from one another after coating. The interior of the chamber achieves high temperatures owing to the melting of metals during coating with the E-beam device, which has a detrimental impact on the lift-off procedure.

The performance of the laser is being improved by decreasing the top contact layer's resistance. Increasing the gold layer thickness is one way to lower the top layer resistance. The gold plating on the P-metal contact in this situation was retained at a thickness level of around 100 nm. The following phase was continuing the metal shielding for a heavier gold coating.

Plating

By removing the lift-off portions and completing a lithography process twice, the gold coating on the upper surfaces of the lasers was thickened using the electroplating method. The front of the laser is connected to an anode (positive) contact. The sample is fully submerged in gold solution, and the cathode (minus) contact is made using a gold ingot. The gold-specific electrons in the gold water and the gold nugget in the cathode are separated and stuck to the sample surface as a result of the current provided, completing the electrical circuit. The coating will accelerate and become less homogenous due to the size of the current driven in this manner.

Metals other than gold are also protected if the cathode metal is not gold in the event that the rate is improperly set. Metal shielding will be made healthy by completing the electroplating phase while taking these factors into account. Using this technique, gold was deposited on the laser surface for 25–30 minutes at a thickness of 4-5 microns.

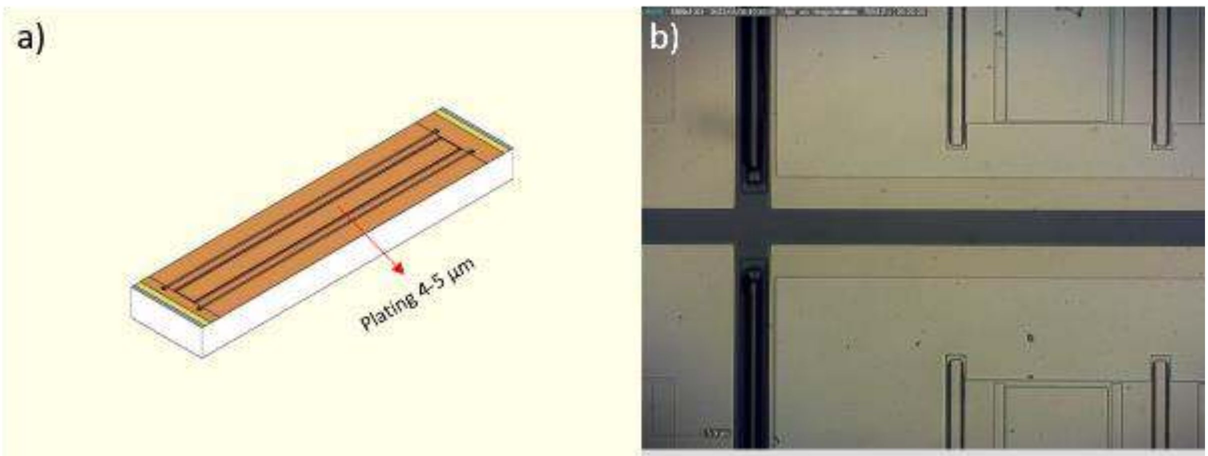

Figure 2-14. a) Schematic view of Au plating from top b) Optical microscope image have been taken with 5X magnification of 4-5 μm gold plating on laser

Back-side Thinning and N-Metal

In order to increase the optical power (W) level that can be obtained from lasers, industrial lasers also use the back-side thinning step, which is one of the final stages of fabrication. Before the back surface of the laser is given the contact (n-metal) feature, the total thickness of 470 µm before fabrication is reduced to approximately 350 µm and below. It is a common technique. In contrast to the solution used in phases like ridge, trench, and cleave, an even more powerful solution was employed to thin the substrate's thickness in order to achieve this feature. Nitric acid and hydrogen peroxide were diluted to create an even more powerful solution, which was intended to swiftly and uniformly erode materials between 100 and 150 um thick.

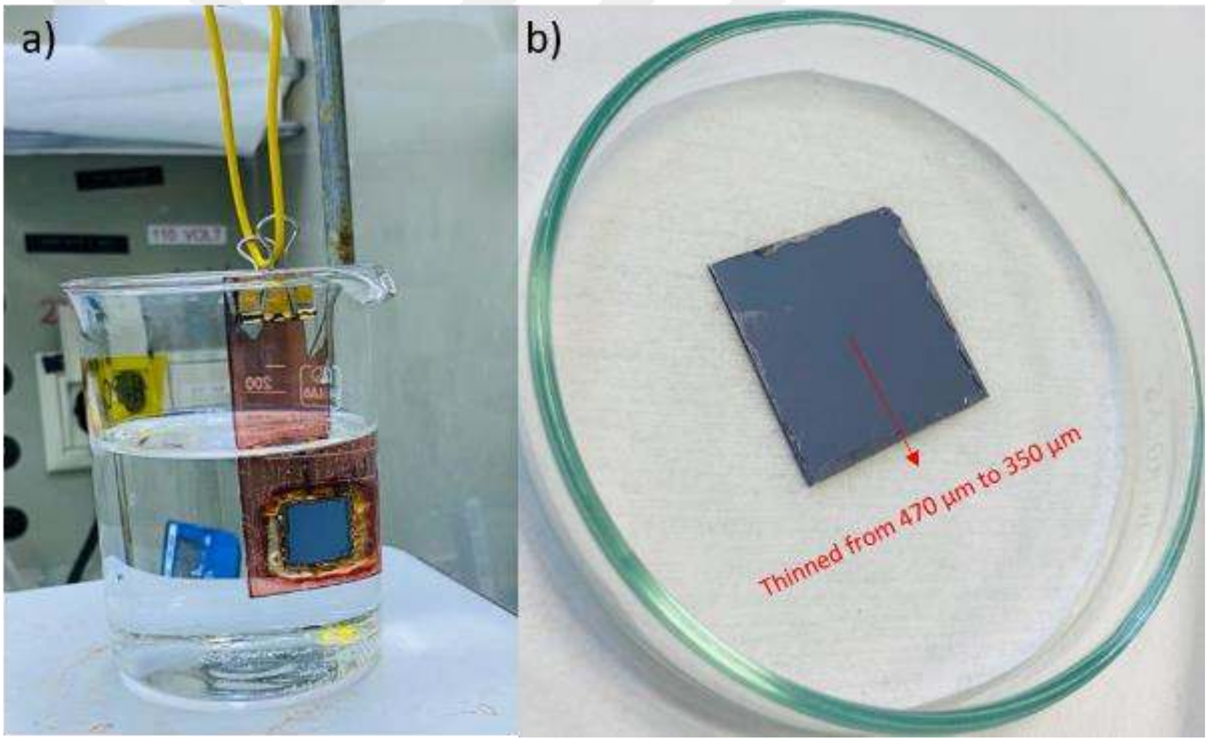

Figure 2-15. a) Schematic view of while sample is back-side thinning b) After thinned the sample around 350 um thick

The fact that P-metal-coated lasers do not harm these surfaces is one of the key aspects at this time. To prevent the solution from penetrating the laser's front surface, which is predicted to leak from the edges, the laser was placed on its front, with the edges covered by photoresist as shown in Figure 2.15. In the above scenario, the problem will be restricted to the lasers' rear surfaces exclusively.

Finally, n-metal is applied to the lasers during the coating process to provide ohmic contact. Coatings of nickel (7.5 nm) and germanium-gold (50 nm) are created, and the RTP (Rapid Thermal Processing) device is used to anneal them. The device is subsequently filled with these two fully annealed metals, which are then re-plated with 500 nm of gold on titanium (40 nm) surfaces. The lasers have been cut and are now prepared for packing.

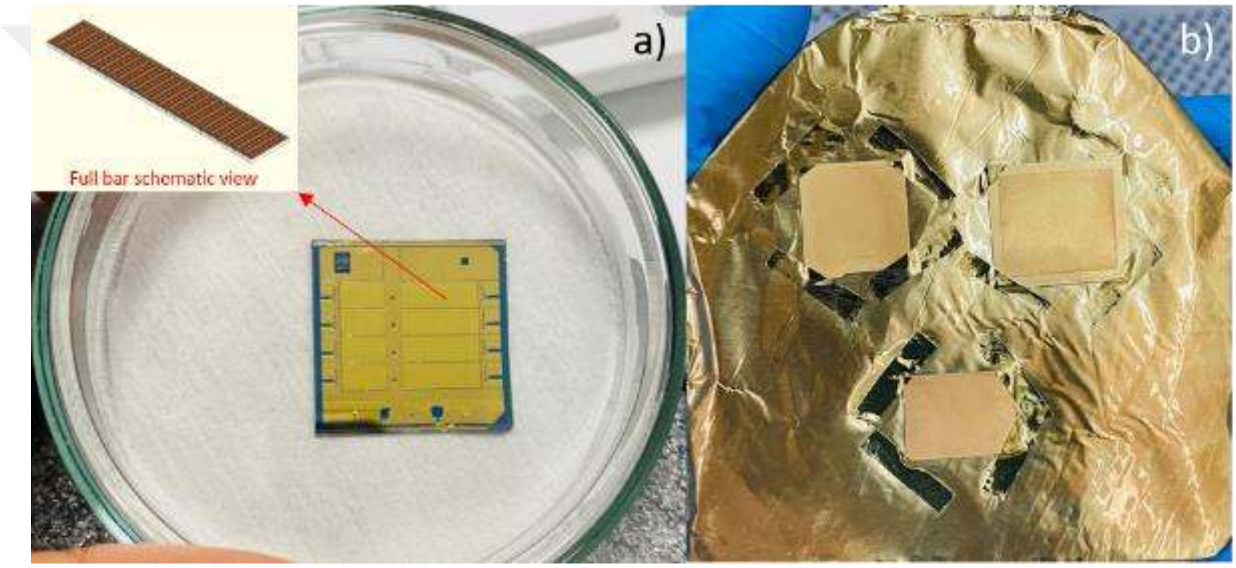

Figure 2-16. Schematic view of N-metal coated of laser bars

2.4 Mirror Coating

The most delicate and sensitive surfaces of semiconductor lasers, the facets, are quickly contaminated by factors like dust and humidity caused by ambient and laboratory conditions during post-fabrication characterization, and they become moistened and oxidized by the oxygen in the space [21],[27]. In the industry, several measures are made to avoid these issues. The facets of the lasers, or the surfaces that function as mirrors following the cleaving step, are subjected to facet passivation before mirror coating.[28]

On the front and rear of the light output surfaces, or facets, of lasers created at the industrial level, several double coatings are made independently in distinct and specialized thicknesses in accordance with the specifications. These coatings are used for a variety of purposes. The light output surfaces are the most delicate and sensitive surfaces that heat up the most while the laser is operating, which is the first of these significant causes [26]. These surfaces are vulnerable to physical processes like COMD (catastrophic optical mirror damage) and COBD (catastrophic optical bulk damage)[29],[30],[24].The laser considerably increases the temperature of the output facet, rendering the mirror inoperable and producing point and localized burn pits on these facets. For the same reason, the laser's internal temperature rises as a result of the structure's severe damage and the photons' incapacity to pass through it healthily. These structures are impacted negatively by the heat load mechanism on a regional level [15].

The impacts of COBD and COMD are much diminished in the lasers where these coatings are realized, and the corresponding lasers' facets are considerably protected. While this effect significantly contributes to the lasers' extended lifespan, it also has a substantial impact on producing consistent light. The laser structure has reduced heat resistance and works more compactly with effective radiation [31].

Another component is to avoid the above-mentioned negative scenarios, extend the lifetime of the lasers we create, and, by working more effectively, concentrate the optical power to be collected from two surfaces into a single surface. One of the surfaces has coatings that give it a high reflectivity, whereas the other only has a single layer of coating, allowing the majority of the light to come from this surface.

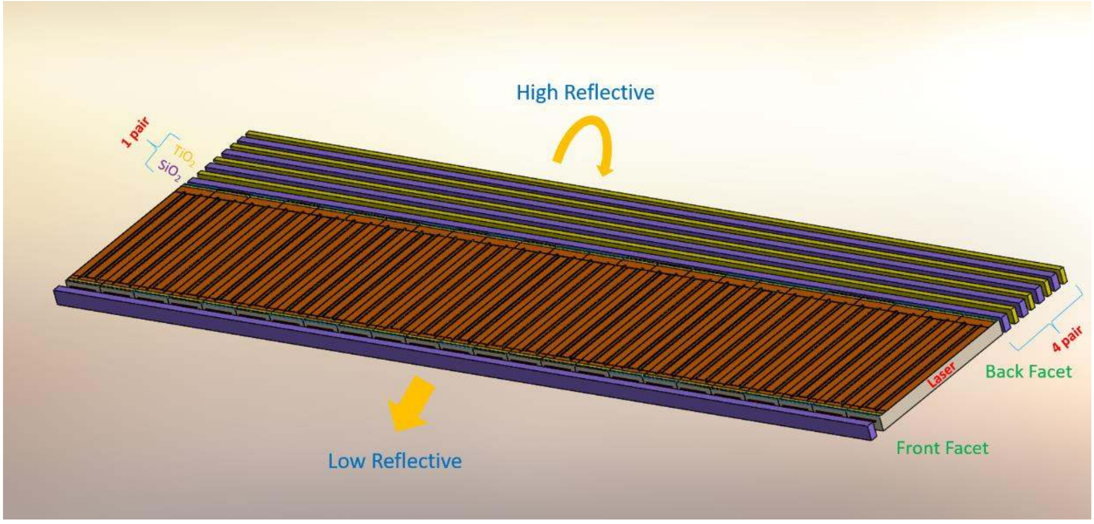

Figure 2-17. Laser Bar Facet's mirror coating schematic view from the side view

Figure 2.17 above provides a visual representation of the coatings applied to the laser bars. The goal is to choose the light's exit surface, give it a low reflectivity rating, and disseminate the light without any more reflection. All photons that reach the rear surface are reflected off it, allowing them to depart through the front surface. The back surface is given a high reflectivity. The materials to be used are chosen in order to obtain the necessary levels of reflection before coatings are applied. In this case, inorganic substances like silicon dioxide and titanium dioxide were used, and it was intended to oxidize the appropriate surfaces [32]. According to the refractive index and layer thickness characteristics previously obtained by simulation results, distinct single layer coatings of these materials were first applied on GaAs and silicon quartz.

The materials to be used are chosen to obtain the necessary levels of reflection before coatings are applied. In this case, inorganic substances like silicon dioxide (SiO_2) and titanium dioxide (TiO_2) were used, and it was intended to oxidize the appropriate surfaces. According to the refractive index and layer thickness characteristics previously obtained by simulation results, distinct thin coatings of these materials were first applied on GaAs and silicon quartz. In the next two tables shows that the optimization of single layer SiO_2 and TiO_2 coatings on GaAs.

Table 2-1. Single layer SiO_2 coating optimization on GaAs

Tooling factor	n (refractive index) (980 nm)	The thickness value on machine thickness monitor (nm)	The real (measured) thickness of Coating (nm)	MSE Value (Ellipsometer)	Coating Method
75	1.4491	100	542	3.71	e-beam
130	1.4669	100	345	2.98	e-beam
250	1.4543	100	195	3.94	e-beam
399.9	1.4643	124	97	0.75	e-beam
399.9	1.4456	157	149	1.88	e-beam
399.9	1.4446	100	136	1.78	e-beam
399.9	1.4459	175	193	4.51	e-beam
399.9	1.4482	135	133	1.13	e-beam

Table 2-2. Single layer TiO_2 coating optimization on GaAs

Tooling factor	n (refractive index) (980 nm)	The thickness value on machine thickness monitor (nm)	The real (measured) thickness of Coating (nm)	MSE Value (Ellipsometer)	Coating Method
75	2.1422	100	581	15.14	e-beam
130	2.2202	100	322	2.74	e-beam
150	2.1548	100	261	6.53	e-beam
260	2.1463	100	159	2.32	e-beam
300	2.1340	100	144	1.94	e-beam
399.9	2.1462	100	106	1.98	e-beam
399.9	2.2037	108	107	1.53	e-beam

The information on how many a pair and layers of these coatings will be coated can be gathered by an optimization based on the measurement results made in a separate device for the reflection values to be obtained, which is done after the optimization of the materials to be coated according to the refractive index and thickness in a single layer is finished. According to the previously specified material and refractive index, the simulation result to calculate the required number of coating pairs is as follows.

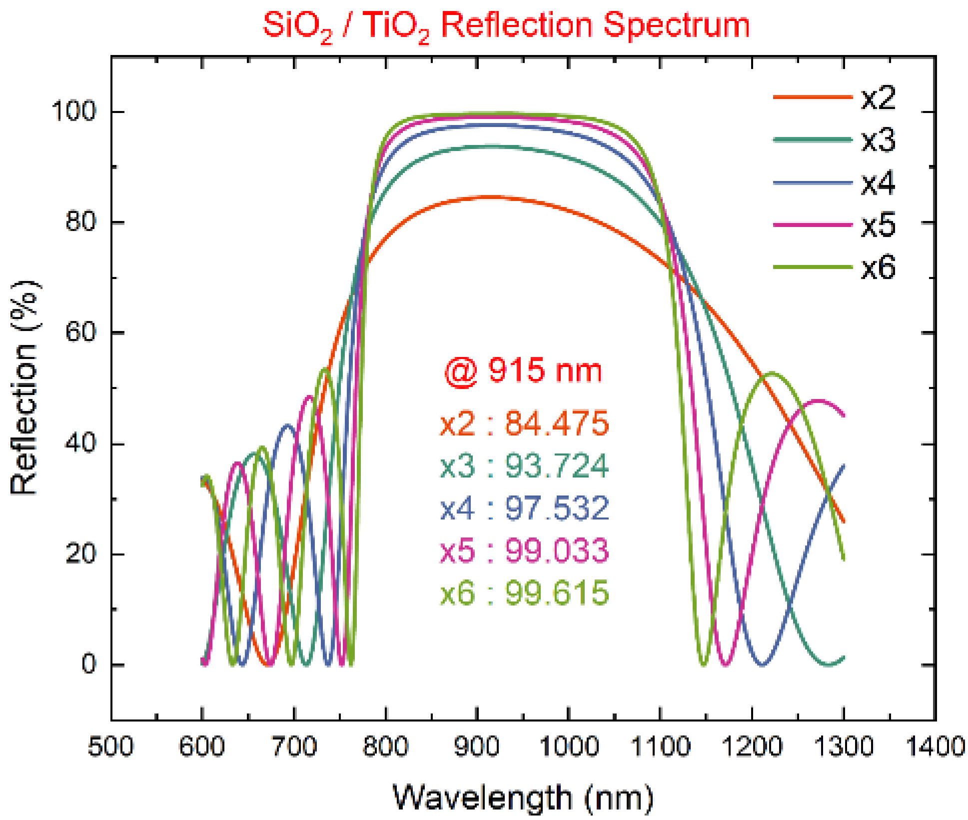

Figure 2-18. Reflection spectrum simulation results for the SiO_2 and TiO_2 according to pair number.

Based on the results of these simulations, it has been discovered that the reflectivity level of 97% can be achieved by applying at least 4 double coatings to one of the lasers' facets. The simulation results will need to be verified by the aforementioned reflectivity measurements in order for this coating to be applied to match those simulation data.

On the other hand, these measurements of SiO_2 and TiO_2 coatings formed in a single layer were also carried out using the Ellipsometer device to demonstrate that the appropriate thickness values are reached by measuring the coating thicknesses. The measurement outcomes from the ellipsometer device are also supplied in order to demonstrate once again that the refractive index values are at the appropriate level using this equipment.

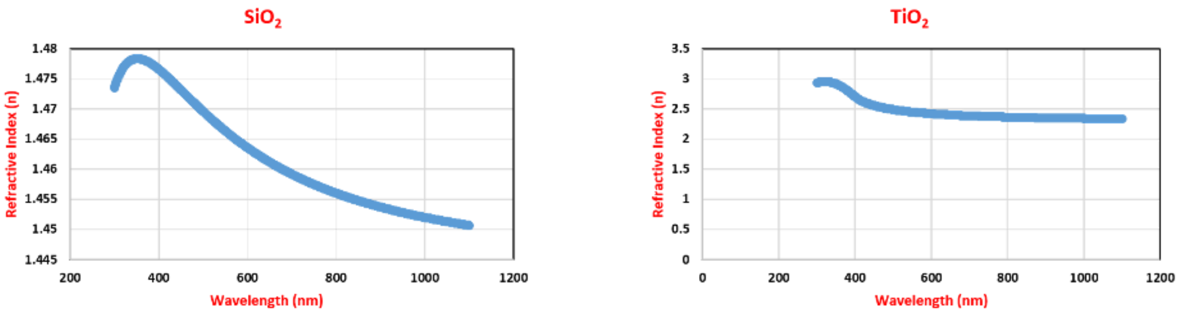

Figure 2-19. Refractive index results of SiO_2 and TiO_2 in ellipsometer device

Based on all of these findings, it was determined that the laser's back facet was coated with 4 pairs of SiO_2 (158 nm) and TiO_2 (108 nm) materials. One layer of SiO_2 covers the facet on the front surface.

The light-emitting surfaces of lasers are referred to as facets in previous part. These facets, which are the main characters in the entire narrative, are estimated to be 370 µm in size when taking the laser's wall thickness into account. This thickness is decreased to 2000 µm at the last step of production. The results are 5 mm or 1 cm long and 200 µm thick if we take each half and complete bar separately. If we see it as a rectangle, we may conceive it to be 5 mm or 1 cm in size, with a short side of 350 µm and a long side that varies depending on whether the laser is a half-bar or a full-bar. Care must be taken to ensure that the coating does not impact any other parts of the laser as the whole coating process is intended to be done just on the facets of the laser. It is crucial that these lasers are positioned properly within the object to be coated in order to ensure that just the necessary parts are covered.

In order to properly position these lasers in the apparatus that will create the coating, an adapter design is required in this direction. The design of the adapter was based on two primary materials, such as coating just the facets of the lasers and shielding the remaining components from the coating generated while within the device, taking into account the chamber and coating quality criteria of the applicable device. The mechanical workshop constructed the adaptor and prepared it for usage when the design was finished.

However, this adapter has been updated as a result of slight modifications to the non-facet portions are, to a lesser extent, exposed to the coating thanks to the E-Beam evaporator device, some challenges in properly positioning the laser’s in the adapter, and finally. Additionally, the new adaptor was created, and coating studies of the coating laser’s facets were completed.

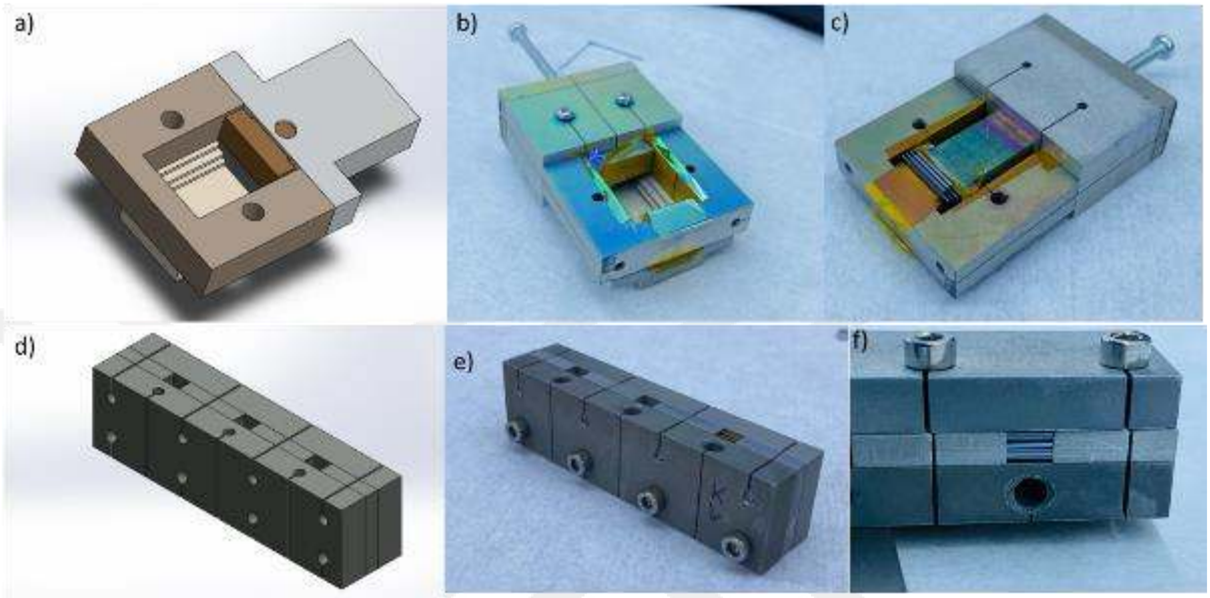

Figure 2-20. a) Schematic view of Design-1 of mirror coating adaptor b,c) The images after manufactured and laser places on Design-1 adaptor d) Schematic view of Design-2 of mirror coating adaptor e,f) The images after manufactured and laser places on Design-2 adaptor

Two distinct designs were created, and as you can see in Figure 2.20 above, lasers were precisely positioned on the pertinent adapters in preparation for being attached to the coating apparatus. The GaAs wafer was sliced and positioned to roughly match the laser’s size as a divider between them. The finished coating will divide the lasers' facets without causing them to stay together in this manner. These wafer structures were therefore made shorter than lasers and fitted into the same adaptor.

Given all of this information, the story-telling coating is completed, and the packaging component is approved. Following the coating, the lasers' facets are carefully checked under a microscope before the packing procedure for the test setup where the lasers will be evaluated and characterized is started.

CHAPTER 3
PACKAGING and TEST SETUP

The mirror coating procedure is finished, and the manufactured lasers are ready for packing. The lasers are divided from one another and packed separately during the cleave process on a 2.5 cm x 2.5 cm wafer to produce a total of 6 distinct bars, comprising 3 pieces 5 mm lasers and 3 pieces 1 cm lasers. Special pens with diamond tips are used to differentiate these lasers from one another. Following the completion of this procedure, each laser is individually examined under a microscope before being glued to copper structures made to correspond with the spot where it will be placed for the test setup. The bonding of the lasers begins after all of the individual lasers' facets, or light-emitting surfaces, are clear and free of any material traces.

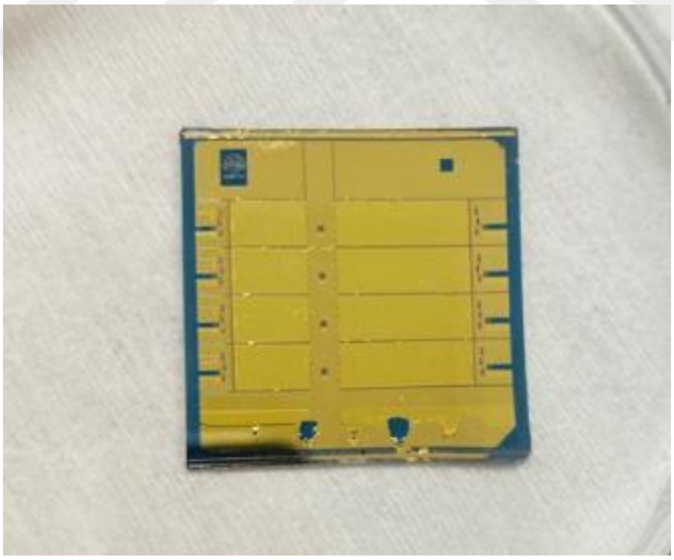

Figure 3-1. The image of fabrication completed bars.

3.1 Packaging of Bar Lasers

Dry nitrogen is used to clean the top surface and facets of the element, removing any wafer debris that may have remained on the lasers' shattered casings during the cleave process or any pieces that may have overflowed onto the element due to the flexible nature of the gold coating. The procedure will be cleaned more thoroughly if it is carried out in a clean room.

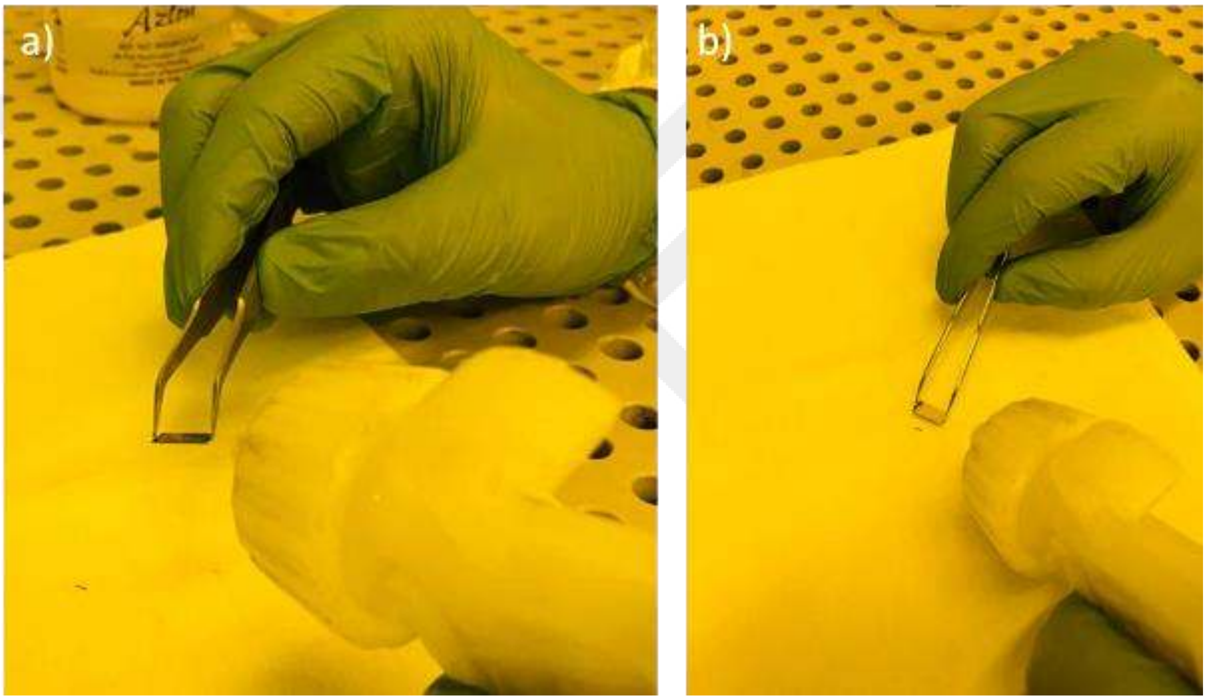

Figure 3-2. Cleaning facet and top part of cleaved bars before bonding

The substance on which the sliced lasers would stick was decided to be copper. Since the laser reaches high temperatures throughout the testing and characterization process, copper is used since it is the best material for heat conduction. The surface is chemically cleansed to eliminate oxidation prior to the treatment. When necessary, these surfaces are also physically treated to reduce roughness. The coppers have been cleaned before packing, as shown in Figure 3.3 below, and are prepared to be packaged.

Figure 3-3. Cleaned copper plates for the laser bonding

As seen in figure 3.4 a, special tweezers are used to identify the placement of the laser bars on these coppers. According to the size of the stencil that will be used to bond the identical lasers, the best gap is chosen. The location where the paste will be put on these coppers will be marked in the subsequent phases by the indium paste that will be applied along this gap. The lasers will be positioned on the paste, which will have been placed to one of these gaps that will be substantially shorter and longer than the size of the lasers.

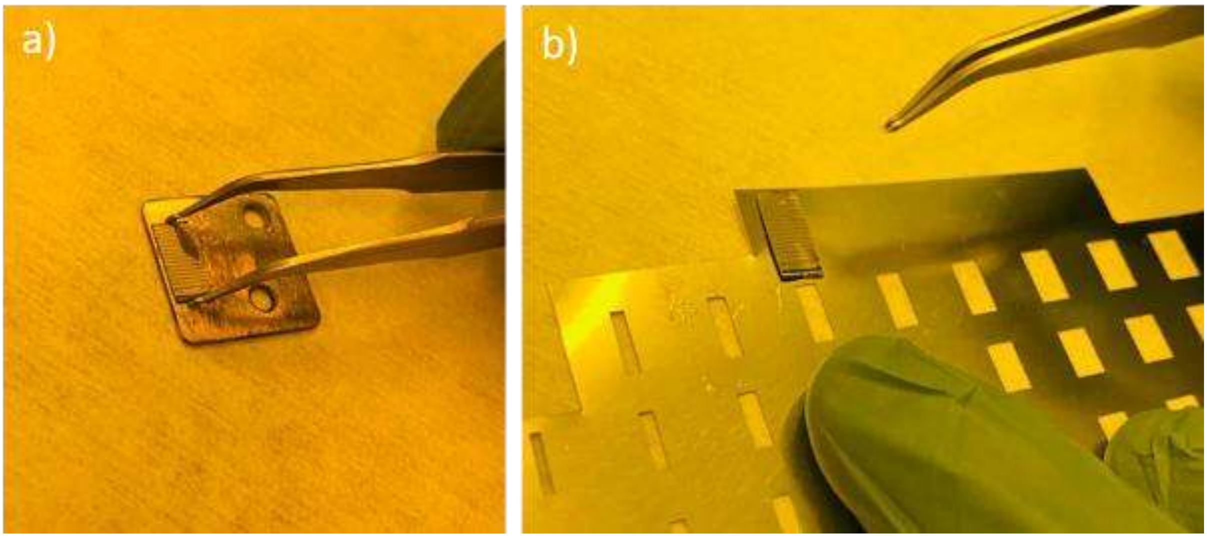

Figure 3-4. a) Alignment of laser on the copper b) Selecting proper size of indium paste region that will be applied at the bottom of the lasers

The laser-sized spot on the copper is lined up with the chosen gap on the stencil. This chamber is filled with indium paste, and the stencil is gently pushed down without moving. All of these steps are shown one by one in Figure 3.5.

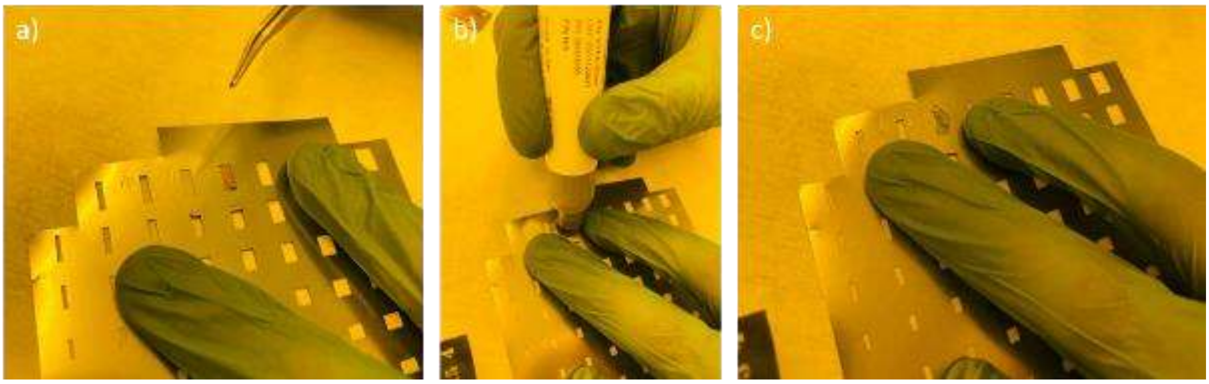

Figure 3-5. a) The image of putting stencil on the copper according to alignment, b, c) Applying indium paste to the selected hole regarding to the laser size

The laser won't adhere properly if the indium paste used to fill the cavity, which is shorter and smaller than the size of the laser, is disordered. As seen in Figure 3.6, this is avoided by removing extra paste using a tiny piece of aluminum sheet and ensuring that the paste on the surface is uniform. This is a crucial element that will guarantee proper laser adhesion. With the paste placed in such a way that the majority of the surface area on the bottom surface of the laser will remain away from the facets, the properly attached laser will transmit the heat conduction to the copper in an accurate manner.

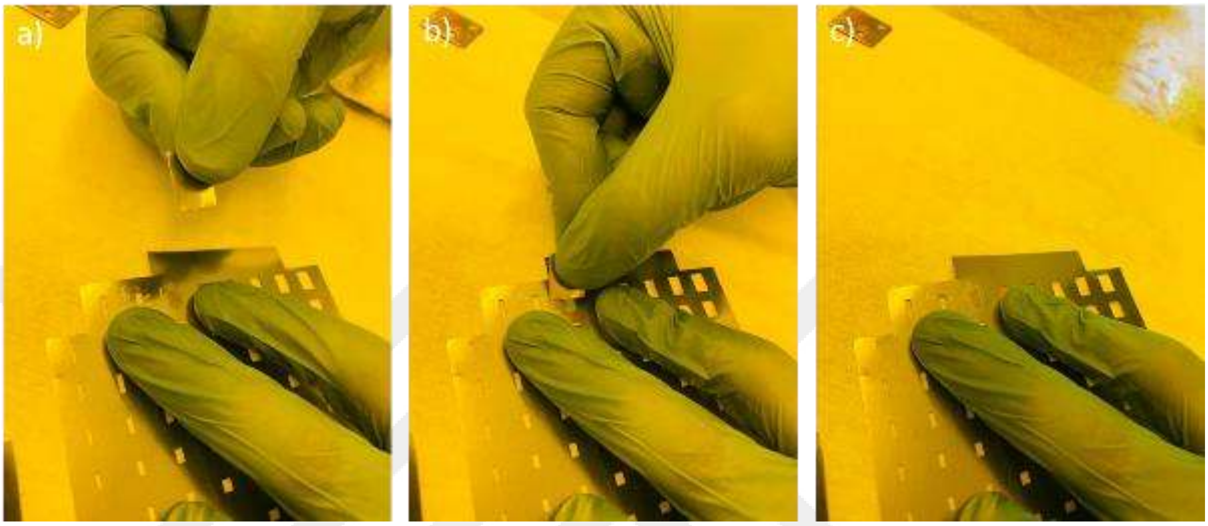

Figure 3-6. a) The view of applied indium paste to the hole, b) Applying sufficient force to the hole to get rid of overdosed indium paste from the hole, c) The view of correct amount of applied paste

With the aid of specialized tweezers, the lasers are then cautiously positioned on the regions where the appropriate size and quantity of indium paste have been deposited. Figure 3.7 depicts how the lasers were positioned on copper. Here, there are two crucial points. The facets must first be taken into consideration while positioning the lasers on these places. This paste cannot be tainted by either aspect. These surfaces, as was previously indicated, are extremely delicate.

Second, when the laser has been applied to the cake, the appropriate force must be manually applied using plastic tweezers with a clean tip. Excessive force that rises from the bottom surface might lead to issues like laser damage or contamination of the facets. Similar to this, insufficient force may prevent the lasers from adhering well and failing to properly transfer the heat produced inside of them to the copper. These factors show that it is crucial to carry out this operation extremely exactly and thoroughly.

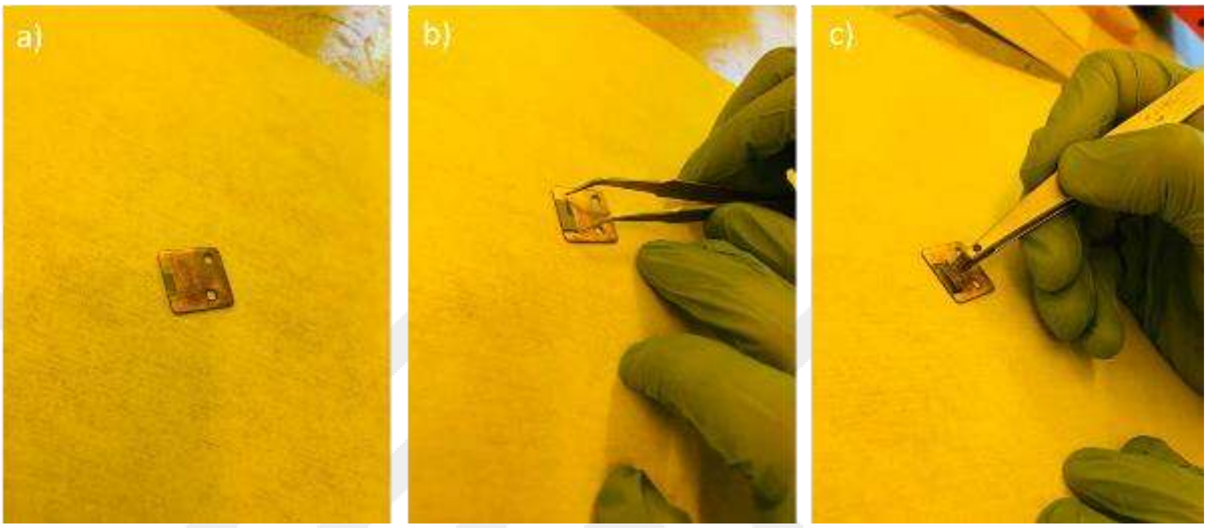

Figure 3-7. a) The view of applied indium paste b) The image of the placing of the bars to the top of the indium applied region of copper, c) The image of applying force to the top of the bar to stick it

Following these steps, the lasers that had remained attached to the copper surfaces had to be baked for 30 minutes at 180^{o}Celsiusdegrees while being optimized in accordance with the guidelines established for the proper adherence of the indium paste. The bars were bagged and prepared for testing after baking. The lasers that have been packed and are prepared for testing are shown in Figure 3.8 below.

Figure 3-8. a) The view of laser bar's on the hot plate, b) the image of ready bar's to test

3.2 Test Setup

All the specifications for the test setup had to be constructed in order to be as similar as feasible to the laser bar test rigs used at the industrial level in order to conduct the tests on the lasers whose packing has been finished. All investigations have been conducted to develop a device near to this level, even if these tests cannot be conducted at the industrial level owing to the limiting circumstances in terms of both equipment and equipment at the laboratory size. First and foremost, in this regard, the selection of the components for the appropriate test setup and their careful purchase have been done. The requirement for the specific manufacture of certain of these parts then developed. The process of procuring and purchasing the necessary parts was started, and the designs for the remaining special manufacturing parts were completed in accordance with their specifications.

To concretely integrate all the pieces for the installation of the appropriate assembly and to confirm the harmony in the integration of the parts to be particularly created with the rest of the system, the entire system was sketched piece by piece using the SolidWorks cat software. Figure 3.9 below in this design provides specifics of the visual, which contains the sections that must be manufactured specifically.

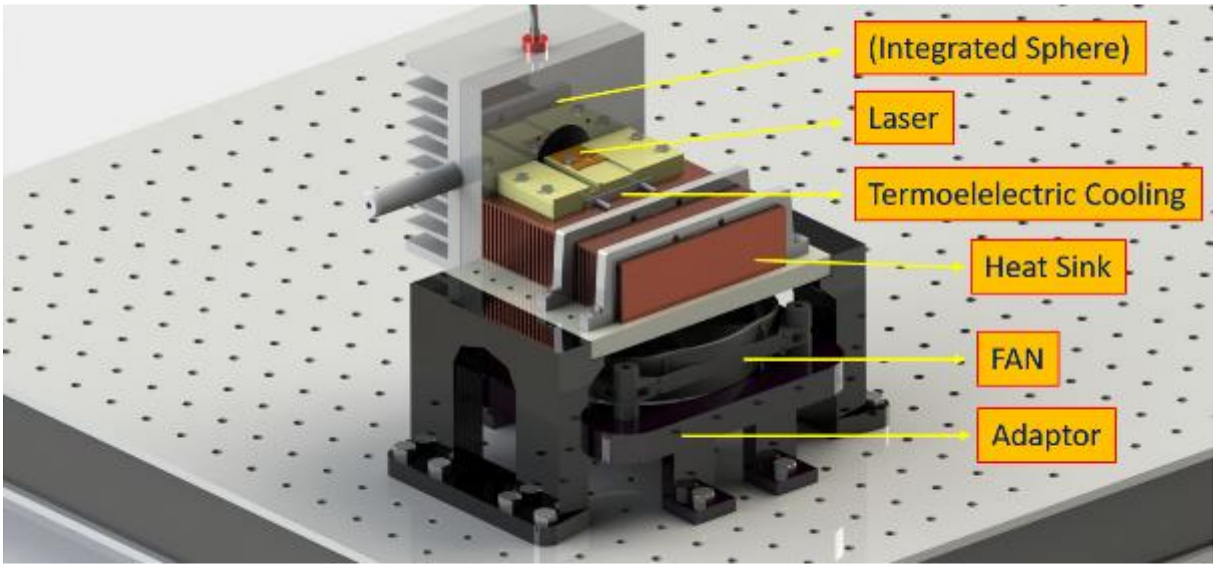

Figure 3-9. Sketching view of test setup

In this instance, as was already mentioned, a high current is applied to the lasers in the test rigs of high-power lasers to dissipate the heat, which is the main drawback of lasers where high powers are obtained by applying a high current to the lasers, and the cooling elements are used intensively due to the requirements of these parts. The heat dissipation is accomplished by applying a high current to the lasers. With the updated technology, it is usually observed that these cooling components are utilized heavily at the industrial level.

In order to evenly spread the heat, the system includes the laser as well as components other than the integrated spherical sections that will be used to measure the power of the beams that will be fired from the laser. It aims to stop the heat produced by the passive cooling approach, which includes the heat sink and fan put in this configuration on the optical table. Figure 3.10 below depicts the assembled picture of the planned components.

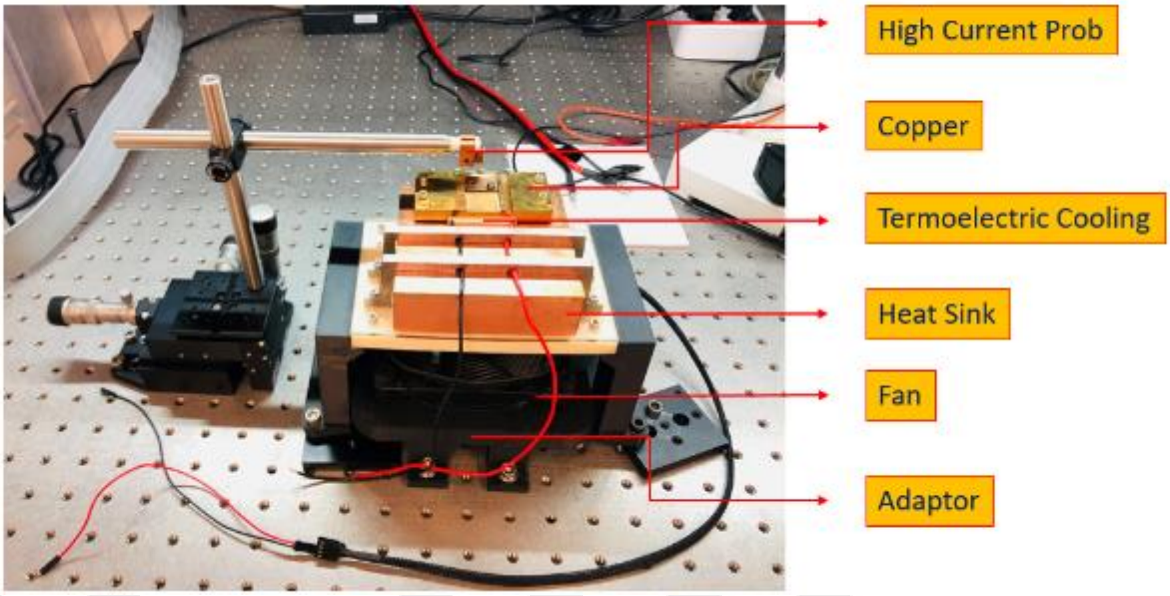

Figure 3-10. The view of installed setup

The fan is designed to remove the heat that has been collected in the heat sink element, as can be seen in Figure 3.11, where the system is examined in more detail. The air ducts of the heat sink portion are intended to remove the high heat that has collected on the rear surface of the thermoelectric cooling component, which is likewise positioned on the heat sink. With the appropriate portion's voltage provided, the front surface of the thermoelectric cooling part was heated up almost to 0^0 degree, and copper was then put to it as illustrated in Figure 3.11.The laser is built into the copper, and the cold surface created by the thermoelectric cooling system is intended to dissipate the heat it generates.

Figure 3-11. Closer look at the heat spreader elements

The requirement for components that will carry the high currents to be driven to the lasers is another prerequisite for laser bar assemblies. In this arrangement, probes that will be required in situations when it is intended to drive a few hundred amperes of current were also required. It was intended to acquire specialized design probes utilized by industrial-size businesses in response to this necessity. However, owing to their exorbitant price, this need was dropped, and research was begun to produce the probes which were essentially learned and thought to be purchased by ourselves utilizing the infrastructure already present in our structure.

The industrial probe for this purpose that inspired Figure 3.12 below was initially created in SolidWorks and then produced in the micromechanical laboratory.

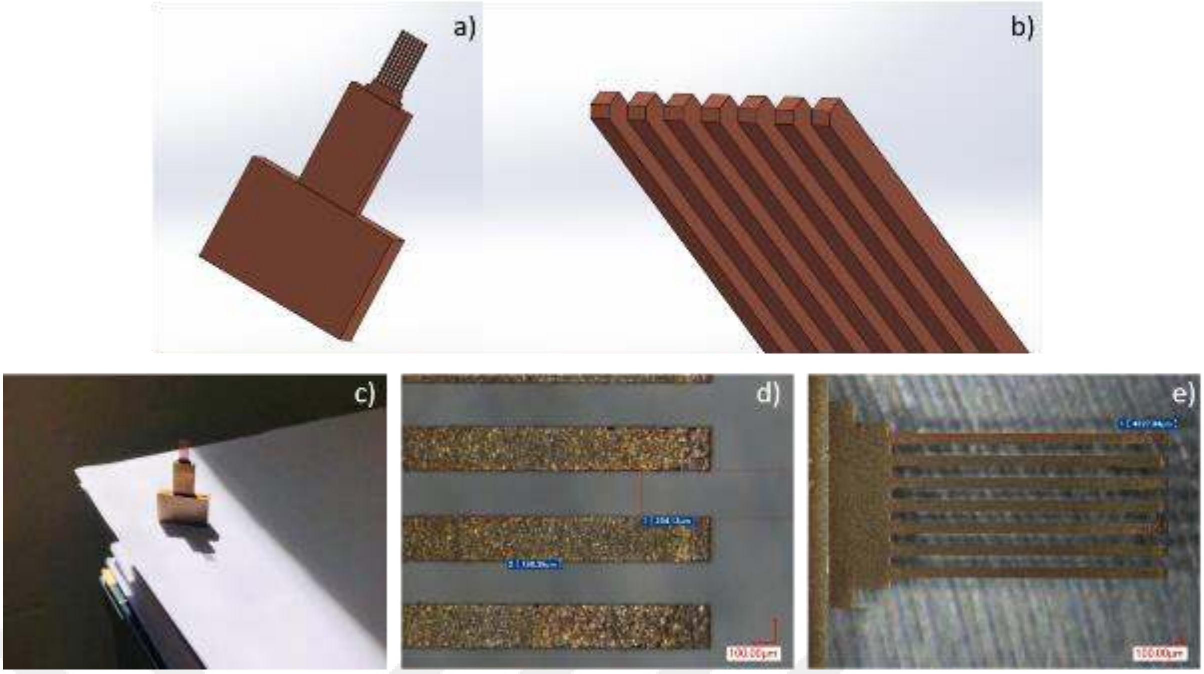

Figure 3-12. a,b) Probe Design-1 schematic view from SolidWorks, c,d,e) The picture of manufactured probe design-1

High heat and current caused the ends of the Design-1 probe, which were quite near to one another and were produced with great accuracy, to gravitate toward one another, which was not viewed as an effective or beneficial outcome. Thus, various probe designs were investigated. Ultimately, after numerous tests and updates, a probe design with eight spring systems was developed, making it more durable than the previous probe. Additionally, by dividing the high current to be driven by eight different probes and dividing the load and heat falling on each probe, an efficient probe was integrated into the system. The graphics for this design and images of it being implemented into the system after it was produced are shown in figure 3.13 below.

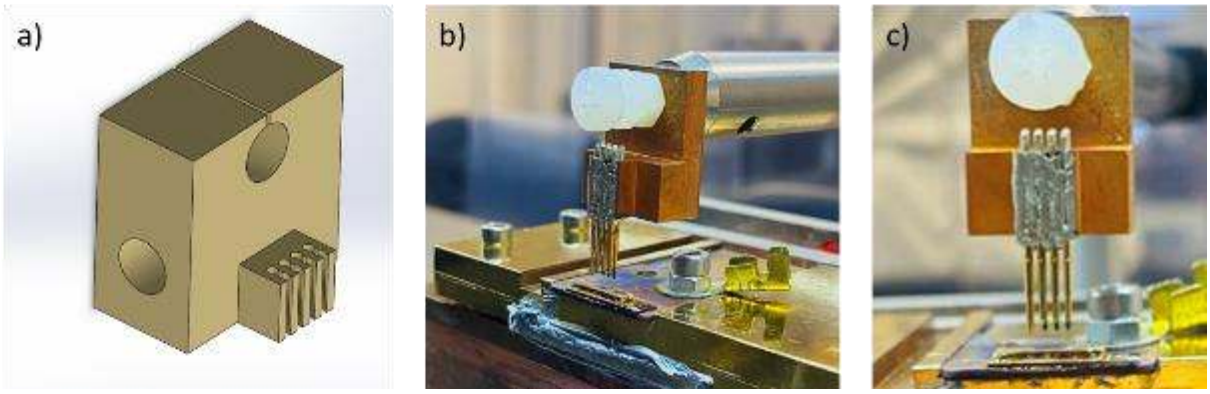

Figure 3-13. a) Probe Design-2 schematic view from SolidWorks, b, c) The picture of manufactured probe design-2

The measurement configuration depicted below was created in accordance with all the technical information previously given, and the test and characterization findings that will be discussed in the next chapter will be presented as data derived from this measurement setup. Before the setup was complete, several revisions were done, some adjustments were made to the defective and missing points, and as a consequence, the following measurement setup was introduced to the lab.

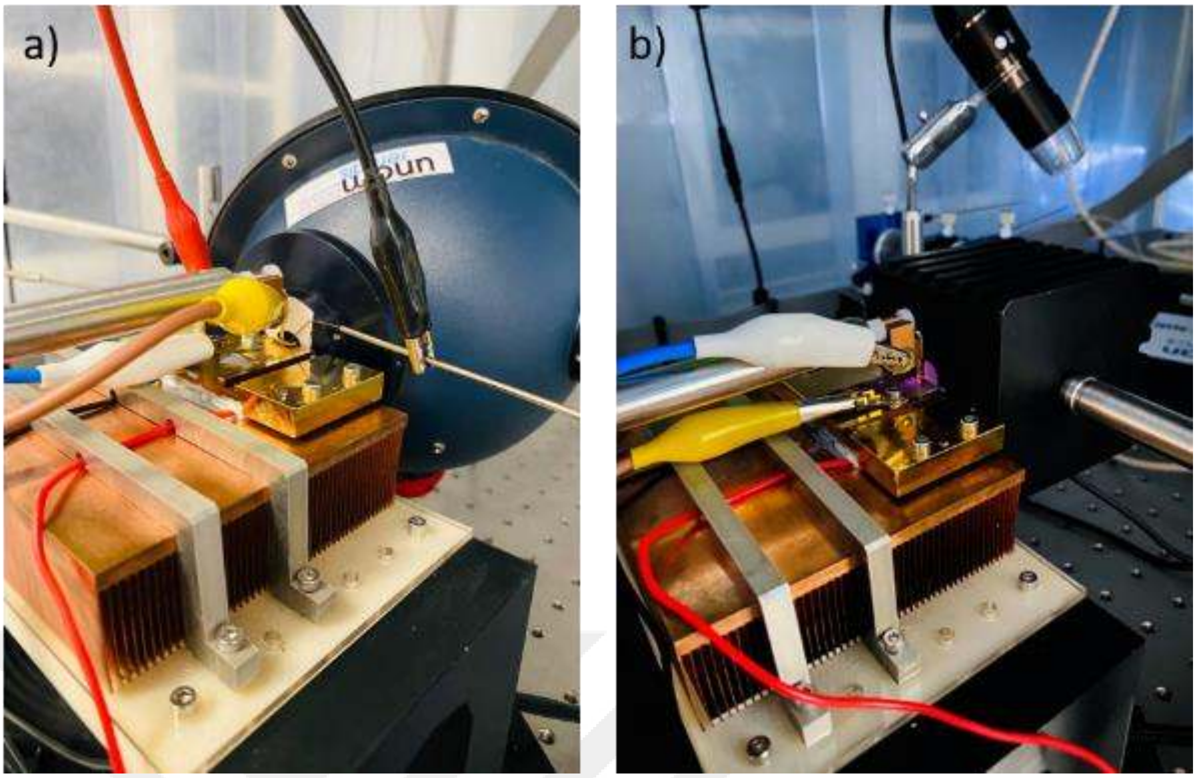

Figure 3-14. The final version of laser bar test setup image

CHAPTER 4
LASER CHARACHTERIZATION RESULTS

The results obtained with high-power semiconductor lasers, which were discussed in detail in the previous chapter, will be presented in detail in this section. The lasers, which were tried to be packaged based on the methods used at the industrial level, were placed in the test setup after they were prepared and ready for testing. The test setup is aimed to perform these tests with devices and equipment suitable for the conditions under which lasers operate at high powers. One of the most important parameters in terms of priority is to ensure that the high temperature generated by these high-power lasers is cooled by the established device and the lasers operate at average temperatures in room conditions. Another parameter is to distribute high currents evenly and homogeneously to all single emitters in the bar structure with appropriate probes. Current-voltage-optical power measurements of these lasers are performed by sensing the radiation by the detector in the correct position.

In this methodology, the measurement findings of single-emitter structures are shown in the graph below, and single laser structures with a length of 5 mm and a cavity width of 190 micrometers produced roughly 16.5 W optical power.

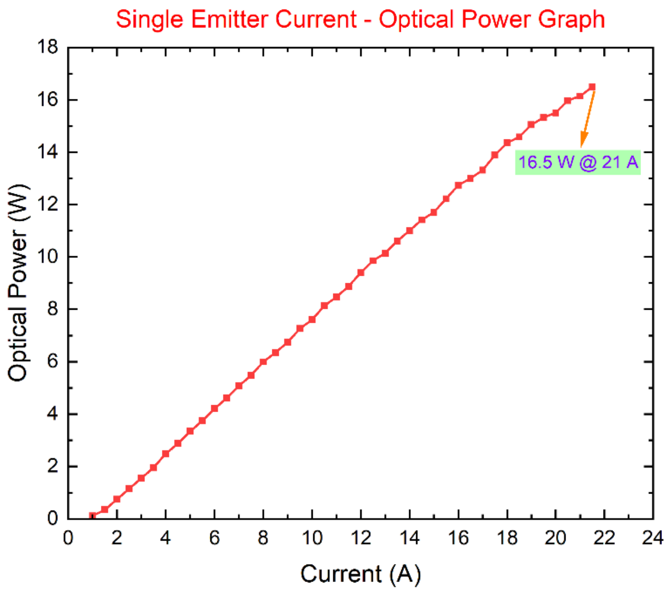

Figure 4-1. Single emitter current-optical power result

Obtaining 16.5 W optical power from a single laser structure, it was discovered that obtaining bars from bar structures, that is, putting single lasers side by side, will greatly surpass the project's need of 100 W optical power.

The following are the post-fabrication measurement data for half (5 mm) and full (1 cm) bar constructions. 11 single emitters were positioned side by side in the half bars, and 24 single emitters were arranged side by side in the whole bar, and their measurements were done identically.

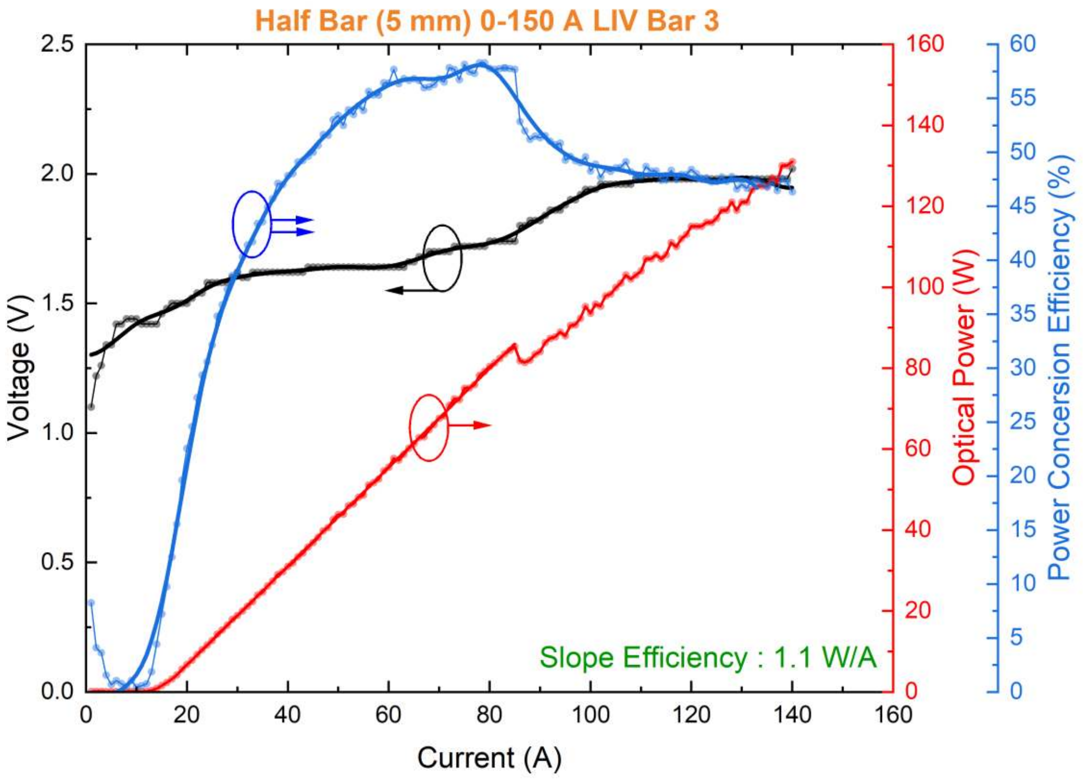

Figure 4-2. Half bar LIV results

As can be seen from the graph, 133 W optical power was obtained from the half-bars in the current range between 0 and 160 A, exceeding the project target of 100 W half-bars. The power conversion efficiency of the related lasers is also around 59% and the slope efficiency is 1.1 W/A. The reason for the small oscillations in the voltage curve is that the voltage is read and recorded manually with the oscilloscope, not directly through the software. While the current is driven by the ILX current source, the voltage is simultaneously obtained and recorded on the laser with the help of probes, which caused these small ripples. Data points were fit, and a smoother graph was obtained.

In the same scenario for the PCE value, the curves were made meaningful with the same method since the voltage was read manually.

At a current level of 87 amperes, approximately 85 W of optical power is obtained, and a small ripple have seen in the curve. Because the Peltier provides cooling during the measurement, the temperature data cannot be read by any temperature control device; therefore, the current fed to the Peltier and thus the cooling system obtained must be done manually. At the 87 amperes current level, the current supplied to the Peltier increased manually, resulting in a small oscillation in the temperature data at this point, which caused a small drop in optical power.

Considering that the trench structures that separate each laser in both half and full bar structures will limit the current applied to the lasers, the trench mask is removed from the fabrication steps and the full process is repeated and the graph comparing the measurement results are as follows.

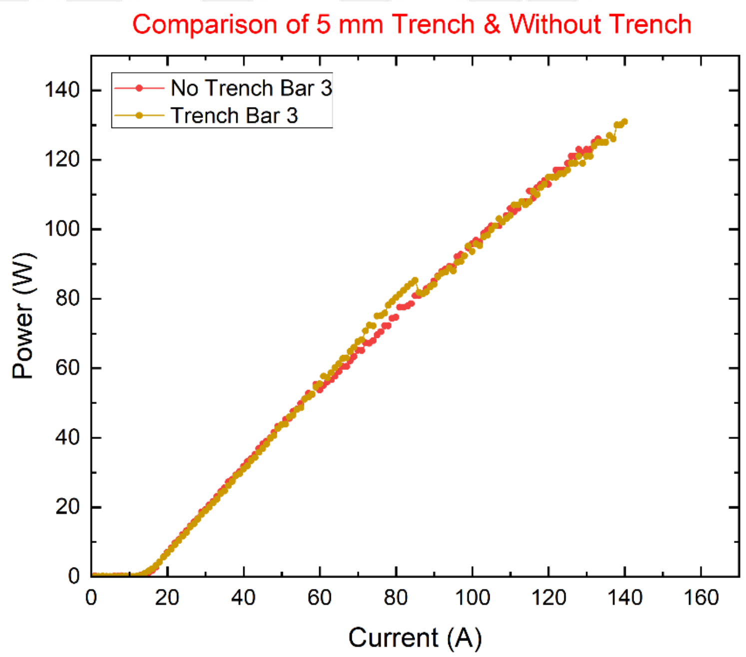

Figure 4-3. Trenched vs. Without Trenched Half bar comparison

From the above graph, it is possible to understand there is no huge difference between making a trench on the laser and not making it. For both, the laser structure gives the same results.

In this context, it was envisaged to obtain approximately two times the power level obtained from half bars from full bars, and the measurements of full bars were measured in the same test setup.

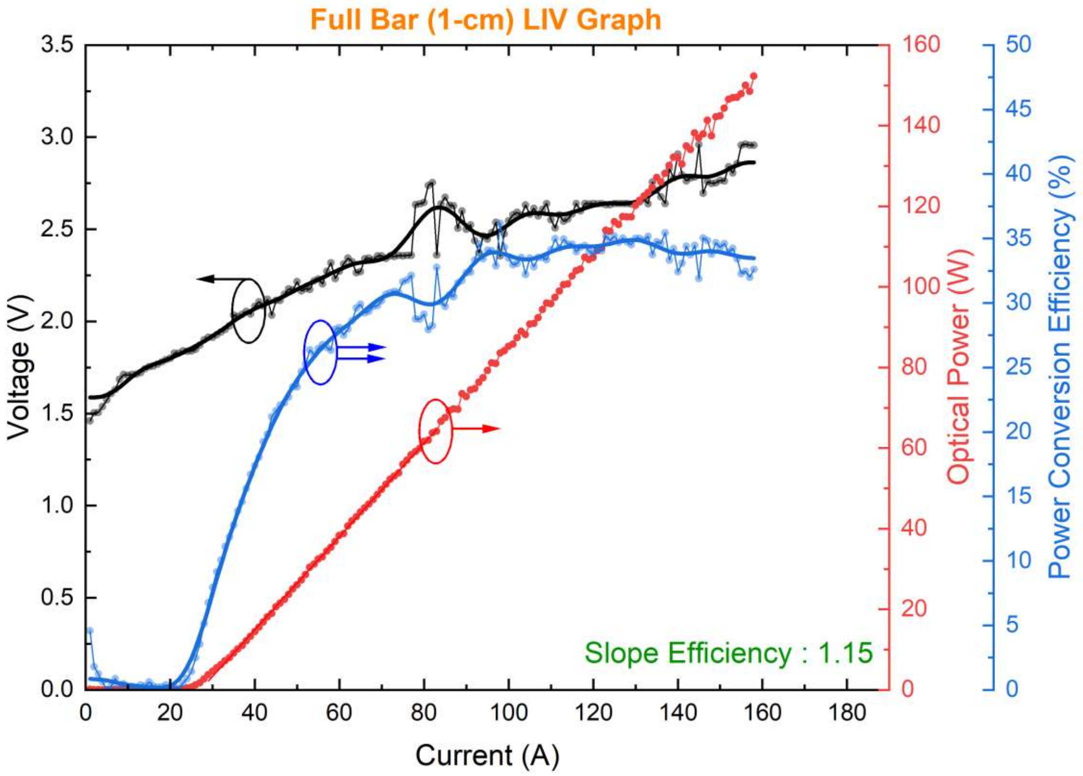

Figure 4-4. 1-cm bar LIV result

The graph proving that approximately 158 W optical power is obtained from full bars is shown in Figure 4.4. Since the current source was limited and the cooling system had to be strengthened, higher currents and therefore powers could not be reached. As can be seen from the graph, the power conversion efficiency was lower than the efficiency of half-bars. Necessary work is being carried out to improve this efficiency, which remains at 35%. In this context, new fabrications are continuing and it is anticipated that future work based on this project will achieve higher power levels with better packaging and mirror coating.

CHAPTER 5
LASER HEATING APPLICATIONS

In the context of this study, high-power laser diodes rather than fiber lasers used in industry for heat treatment on materials like glass, etc. High power diode laser bars were designed and fabricated by positioning a FAC lens (fast axis collimator) in front of the facets to keep the beam at the order of 100 µm and perform this process with a more intense light intensity on the material to be heat treated and associated materials[33].

Due to the strength of the beam and the fact that it is around 100 µm, the employment of fiber lasers in recent research has raised interest in this area[13]. The efficiency is down to 30% due to losses in the laser's coupling step to the fiber. The criteria can be met by utilizing high-power diode laser bars with a lens in front of them to provide collimation in such heat treatment applications as the use of high-power laser bars with low losses in place of these will contribute to increasing the efficiency up to 60%.

The degree of heat treatment on the glass surface has been attained with the manufactured half and full bars, which are comparable to the research indicated in the preceding sections with different samples.

On 5 cm X 5 cm soda lime glass given by Şişecam, another project partner, various heat treatment tests were conducted in this approach. It is intended to heat treat the silver layer that has been deposited if only a single coating of silver has been applied to the top surfaces of the pertinent glasses using laser beams that are emitted from the facets of the lasers. Following the heat treatment, it is envisaged that the heat treatment will be deemed effective if the anticipated values are attained for a few Şişecam-set criteria.

The test strategy was first realized before the pertinent tests could be executed. To collect the data where the influence of each parameter to be applied on various glasses can be seen clearly, a test matrix was built, along with tables and parameters. This test matrix and the information to be gathered from the heat-treated glasses are shown in the table below.

Table 5-1. Test data for thermal processing

Test	Laser Power [W]	CW/ QCW	Scanning Speed [mm/s]	Laser - Glass Distance [mm]	Tvis [%]	Haze	Surface Resistivity	Emissivity
1	94	CW	5	20	51.1	2.75	10.95	0.035
2	75	CW	5	20	52.8	0.44	3.96	0.029
3	50	CW	5	20	52.7	0.4	4.131	0.031
4	150	QCW	5	20	52	0.3	4.514	0.035
5	100	QCW	5	20	51.4	0.3	4.332	0.04
BeforeTemper (without laser)	Base Values				51.3	0.3	4.31	0.04
After Temper (without laser)	Target Values				55.6	0.38	3.49	0.028

The relevant table's test row specifies the heat treatment order that should be utilized on five different glass surfaces. It plans to do many checks on each glass. In this process, the data that will ensure a safe and accurate heat treatment technique will be identified, and these data will be chosen as reference data, and the testing conditions for various glasses will be developed.

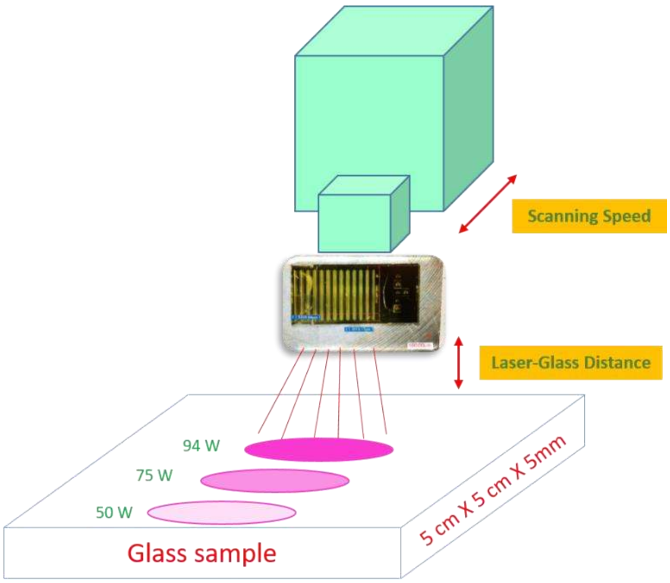

Figure 5-1. Glass heating process setup

It was determined during the evaluation of the laser power difference that the heat treatment would be achieved with the heat that would arise with the applied power by applying optical power to each glass at varying powers. It is meant to begin with high power and has a starting power of roughly 94 W. It is intended to decline to 50 W optical power levels from these levels and thermally treat the silver layer with heat produced by these levels of power.

It is intended to examine the differences between the CW and QCW parameters by carrying out the necessary tests in both situations and operating the laser under both continuous current and pulsed current settings. These two test scenarios were developed to investigate how this variation will directly impact the heat treatment process since the heating of the lasers will change in the two different cases.

It was thought reasonable to begin at a speed of 5 mm/s for the scanning speed. It is crucial to establish the scanning rates of the relevant tests since this parameter, along with optical power, is one of the most crucial ones in the heat treatment process. The need that the 3-axis micromanipulator (stage) portion, where the lasers will be allowed to travel in 3 axes in the test setup, to be electro-motorized, is critical to determining these speeds. The precise speed and uninterrupted movement of the lasers with the appropriate micromanipulators is a crucial element that will impact the heat treatment process. It is crucial that the heat produced by the optical power from the laser in the relevant surface area is sufficient in this regard since the heating of the glass surface in the square millimeter region will change every second after the accurate assessment of the speed. Slow scanning rates will result in many scenarios, such as optical or physical flaws on the surface owing to excessive heat on the surface, while quick scanning speeds will prevent lasers from sufficiently heating the appropriate area. In this regard, the most precise measurement of this speed is crucial for heat treatment.

The proximity-distance measurements between the lasers and the surface that has to be heated up are another factor [34].The correct determination of the relevant distance is directly correlated with the scanning speed; if the relevant distance is too close to the surface at the determined scanning speeds, it may still cause damage even if the speed is accurate, whereas the excessive distance creates circumstances where two interrelated parameters have a say, such as inadequate heat treatment even if the speed is slow. In this situation, the significance of the space permitted by the test setup between the lasers and the glass surfaces increases.

One of the crucial factors taken into account by glass makers during heat treatment testing is the T_{vis} value. This value, which expresses the transparency value in the visible region of the spectrum, is significant because it must be obtained in accordance with the specifications and because it affects the glass's ability to produce clear images and is another factor to be taken into account during heat treatment tests.

The haziness of the glass surface is described by the haze parameter. T_{vis} value, for example, is a value that, upon heat treatment, has a direct bearing on the glass's ability to produce images. The image will be hazy and an excessive heat treatment scenario will take place if the haze value is read over the criteria.

Since the related glasses include a silver coating, the surface resistance value needs to be a crucial consideration in this heat treatment. It has become crucial to maintain the resistance level at the required level because low surface resistance makes it easier to physically process the glass surface following heat treatment.

As the criterion for the propagation of the rays arriving from the visible zone on the glass surfaces, the final characteristic in the table, emissivity, is chosen. Since the picture after the glass surfaces are heat-treated is transmitted correctly and the emissivity value is at the necessary levels in the measurements, this value stands out as a characteristic that will directly affect the image quality.

The glasses are heated throughout the appropriate silver-plating process, or "tempered." The base value for each parameter is established, as shown in the table, and the same values are tested once again after tempering to verify if the necessary conditions are satisfied on the heat-treated glass surface. To be employed in the heat treatment process, constants are created from the values that are near the goal values as determined by Şişecam and the test scenario.

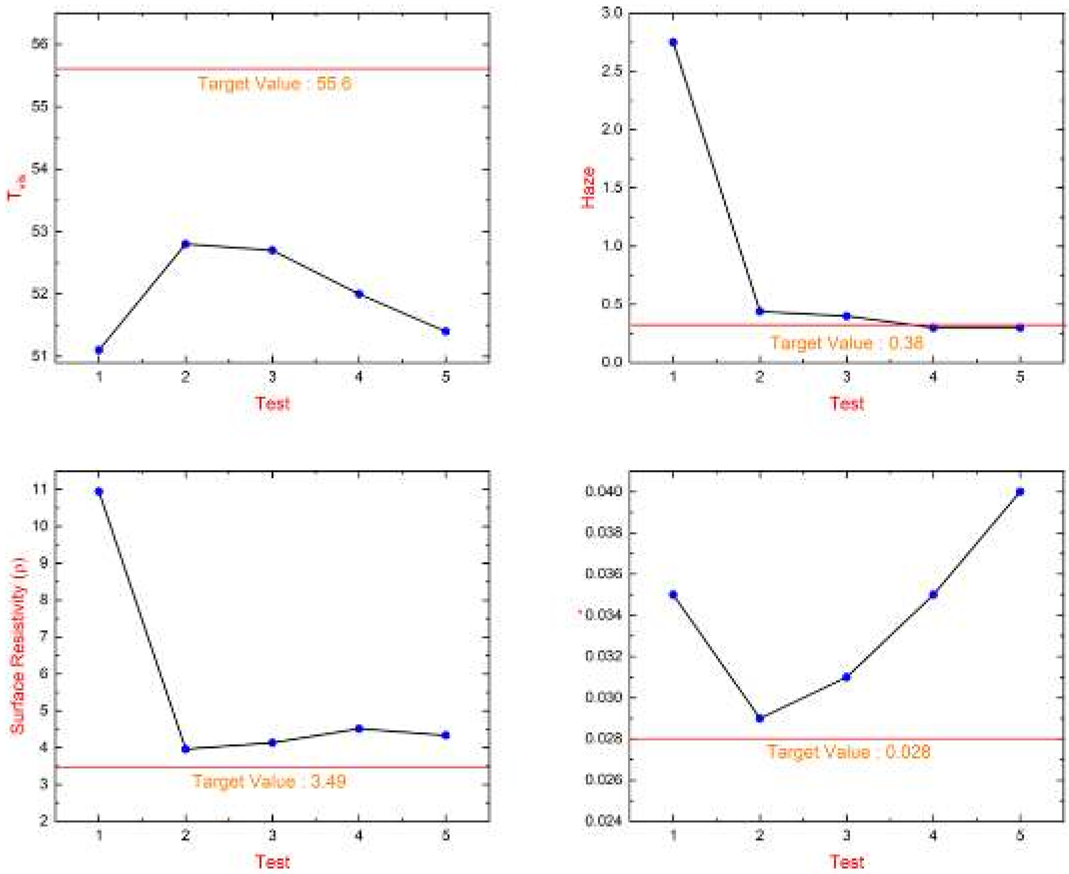

Figure 5-2. Thermal processing graphics for the parameters. In this manner the data point which is close to the target values will be proper for the best test condition scenario.

By looking for the condition of closeness to the desired values, the results of the heat treatment tests conducted while taking into account each parameter established in accordance with the table were obtained visually. By prioritizing the next test conditions after ensuring that each value complies with the criteria, these graphs offer light on the heat treatment tests that need to be performed with new values.

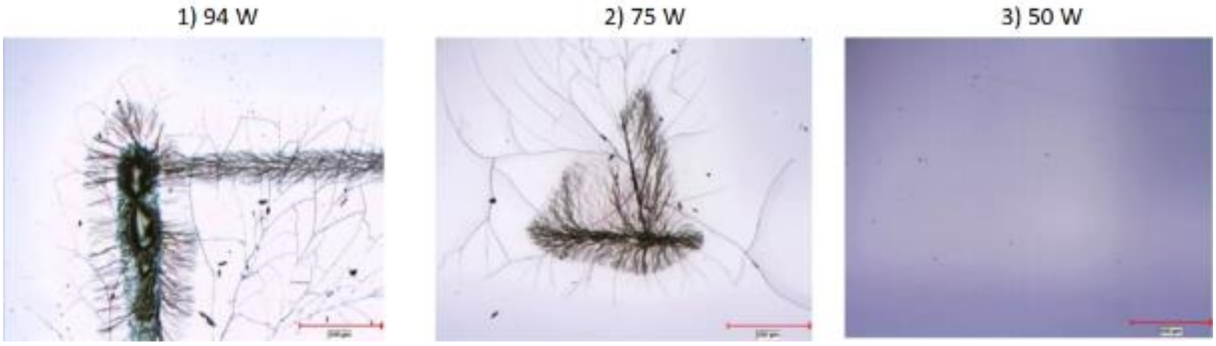

Figure 5-3. Optical microscope images produced after heat treatment with various laser powers on coated glass surfaces at a scanning speed of 5 mm/s and a distance of 20 mm.

Figure 5-17 demonstrates images of the glass surfaces observed under a microscope following heat treatment using heat produced by 94 W, 75 W, and 50 W optical powers on various glass surfaces, respectively. Test conditions included a scanning speed of 5 mm/s and a distance of 20 mm between the lasers and the glass surfaces. The glass surfaces heated by lasers running on a continuous current source had various flaws, as seen in the first two images. The parameters of optical power, laser-glass distance, and scanning speed are many combinations that result in the production of these flaws. For carrying out the tests again, a new standard threshold value was chosen for each parameter, and Table 1's test plan was modified.

5.1 Conclusion and Outlook

Within the scope of the TÜBİTAK-1004 project, the fabrication of high-power semiconductor lasers and the tests of these lasers have been completed, and 132 W of optical power has been obtained from half bars and 158 W from full bars. With these power values, the 100 W optical power target of the project has been achieved. Intensive efforts were also made for the mirror coating of these lasers, and the optimization process was completed. Although the mirror coating was partially performed due to a problem with the device being coated, no results reflected in the tests were obtained.

On the other hand, parameters such as the working conditions and test setup of the lasers to be used in the heat treatment process were determined, and the first test results were completed. A new mask design was completed for both mirror coating of the lasers and the lasers to be packaged under industrial conditions to be used in heat treatment processes, and more than 40 laser bars were fabricated with these masks.

In the later stages of the project and this study, the fabricated lasers will be mirror coated by an industrial partner and then packaged under industrial conditions. Thanks to this packaging and mirror coating, test results can show that efficient high-power lasers can be obtained. These packaged lasers can be included in the process to be used in heat treatment by completing all characterizations under determined test conditions. The following process is targeted for the realization of heat treatment processes using these lasers instead of large-scale furnaces.

REFERENCES

[1] A. E. Siegman, *Lasers*. University science books, 1986.

[2] R. Menzel, *Photonics: linear and nonlinear interactions of laser light and matter*. Springer Science & Business Media, 2013.

[3] E. Şeker *et al.*, "Single-mode quasi PT-symmetric laser with high power emission," *Light: Science & Applications,* vol. 12, no. 1, p. 149, 2023.

[4] H. Sun, *A practical guide to handling laser diode beams*. Springer, 2015.

[5] L. A. Coldren, S. W. Corzine, and M. L. Mashanovitch, *Diode lasers and photonic integrated circuits*. John Wiley & Sons, 2012.

[6] Y. X. Liu *et al.*, "High-power operation and lateral divergence angle reduction of broad-area laser diodes at 976 nm," (in English), *Opt Laser Technol,* vol. 141, Sep 2021, doi: ARTN 10714510.1016/j.optlastec.2021.107145.

[7] Y. Lan *et al.*, "808 nm broad-area laser diodes designed for high efficiency at high-temperature operation," (in English), *Semicond Sci Tech,* vol. 36, no. 10, Oct 2021, doi: ARTN 10501210.1088/1361-6641/ac2160.

[8] Y. L. Zhao *et al.*, "Epitaxially-Stacked High Efficiency Laser Diodes Near 905 nm," (in English), *Ieee Photonics J,* vol. 14, no. 6, Dec 2022, doi: Artn 155700610.1109/Jphot.2022.3211964.

[9] A. Demir, M. Peters, R. Duesterberg, V. Rossin, and E. Zucker, "Semiconductor Laser Power Enhancement by Control of Gain and Power Profiles," (in English), *Ieee Photonics Technology Letters,* vol. 27, no. 20, pp. 2178-2181, Oct 15 2015, doi: 10.1109/Lpt.2015.2455975.

[10] Y. X. Liu *et al.*, "48 W Continuous-Wave Output From a High-Efficiency Single Emitter Laser Diode at 915 nm," (in English), *Ieee Photonics Technology Letters,* vol. 34, no. 22, pp. 1218-1221, Nov 15 2022, doi: 10.1109/Lpt.2022.3207786.

[11] X. Liu, W. Zhao, L. Xiong, and H. Liu, *Packaging of high power semiconductor lasers*. Springer, 2015.

[12] P. W. Epperlein, *Semiconductor laser engineering, reliability and diagnostics: a practical approach to high power and single mode devices*. John Wiley & Sons, 2013.

[13] E. Zucker *et al.*, "Advancements in laser diode chip and packaging technologies for application in kW-class fiber laser pumping," in *High-Power*

Diode Laser Technology and Applications XII, 2014, vol. 8965: SPIE, pp. 38-51. [14] P. Crump *et al.*, "Efficient high-power laser diodes," *IEEE Journal of Selected Topics in Quantum Electronics,* vol. 19, no. 4, pp. 1501211-1501211, 2013.

[15] Y. X. Liu *et al.*, "Elimination of catastrophic optical mirror damage in continuous-wave high-power laser diodes using multi-section waveguides," (in English), *Opt Express,* vol. 30, no. 18, pp. 31539-31549, Aug 29 2022, doi: Artn 46186610.1364/Oe.461866.

[16] Y. Karni *et al.*, "Active cooling solutions for high power laser diodes stacks - art. no. 687604," (in English), *P Soc Photo-Opt Ins,* vol. 6876, pp. 87604-87604, 2008, doi: Doi 10.1117/12.765156.

[17] S. McDougall *et al.*, "Advances in diode laser bar power and reliability for multi-kW disk laser pump sources," in *High-Power Diode Laser Technology XVIII*, 2020, vol. 11262: SPIE, pp. 30-38.

[18] V. Rossin *et al.*, "High power, high brightness diode lasers for kW lasers systems," in *2015 IEEE High Power Diode Lasers and Systems Conference (HPD)*, 2015: IEEE, pp. 35-36.

[19] P. Crump and G. Tränkle, "A brief history of kilowatt-class diode-laser bars," in *Novel In-Plane Semiconductor Lasers XIX*, 2020, vol. 11301: SPIE, pp. 148-156.

[20] K. Kleine and P. Balu, "High-power diode laser sources for materials processing," in *2017 IEEE High Power Diode Lasers and Systems Conference (HPD)*, 2017: IEEE, pp. 3-4.

[21] H. Li *et al.*, "High-efficiency, high-power diode laser chips, bars, and stacks," in *High-Power Diode Laser Technology and Applications VI*, 2008, vol. 6876: SPIE, pp. 140-145.

[22] M. Peters, V. Rossin, M. Everett, and E. Zucker, "High-power high-efficiency laser diodes at JDSU," in *High-Power Diode Laser Technology and Applications V*, 2007, vol. 6456: SPIE, pp. 141-151.

[23] H. Wenzel, P. Crump, A. Pietrzak, X. Wang, G. Erbert, and G. Tränkle, "Theoretical and experimental investigations of the limits to the maximum output power of laser diodes," *New Journal of Physics,* vol. 12, no. 8, p. 085007, 2010.

[24] H. Naito *et al.*, "Long-term reliability of 915-nm broad-area laser diodes under 20-W CW operation," *IEEE Photonics Technology Letters,* vol. 27, no. 15, pp. 1660-1662, 2015.

[25] P. Crump *et al.*, "20W continuous wave reliable operation of 980nm broad-area single emitter diode lasers with an aperture of 96um," in *High-Power Diode Laser Technology and Applications VII*, 2009, vol. 7198: SPIE, pp. 315-323.

[26] Y. Wang, H. Qu, Y. Wang, F. Dong, Z. Chen, and W. Zheng, "Radio Frequency Plasma-Enhanced Reactive Magnetron Sputtering Deposition of α-SiN x on Photonic Crystal—Laser Diodes for Facet Passivation," *ACS omega,* vol. 4, no. 23, pp. 20205-20211, 2019.

[27] P. Ressel *et al.*, "Novel passivation process for the mirror facets of Al-free active-region high-power semiconductor diode lasers," *IEEE Photonics Technology Letters,* vol. 17, no. 5, pp. 962-964, 2005.

[28] Y. Lan, G. W. Yang, Y. L. Zhao, Y. X. Liu, and A. Demir, "Facet passivation process of high-power laser diodes by plasma cleaning and ZnO film," (in English), *Appl Surf Sci,* vol. 596, Sep 15 2022, doi: ARTN 15350610.1016/j.apsusc.2022.153506.

[29] A. Demir *et al.*, "COMD-free continuous-wave high-power laser diodes by using a multi-section waveguide method," in *High-Power Diode Laser Technology XXI*, 2023, vol. 12403: SPIE, pp. 86-93.

[30] K. Ebadi *et al.*, "Multisection waveguide method for facet temperature reduction and improved reliability of high-power laser diodes," in *Semiconductor Lasers and Laser Dynamics X*, 2022, vol. 12141: SPIE, pp. 12-20.

[31] S. Arslan, S. Gündoğdu, A. Demir, and A. Aydınlı, "Facet cooling in high-power InGaAs/AlGaAs lasers," *IEEE Photonics Technology Letters,* vol. 31, no. 1, pp. 94-97, 2018.

[32] Z. Tahir *et al.*, "Highly Reflective Distributed Bragg Reflectors for Planar Microcavities: From Modelling to Experimentation," *Transactions on Electrical and Electronic Materials,* pp. 1-8, 2023.

[33] M. Zavala-Arredondo *et al.*, "Laser diode area melting for high speed additive manufacturing of metallic components," *Materials & Design,* vol. 117, pp. 305-315, 2017.

[34] K. Mumtaz and N. Hopkinson, "Selective laser melting of thin wall parts using pulse shaping," *Journal of Materials Processing Technology,* vol. 210, no. 2, pp. 279-287, 2010.

CURRICULUM VITAE

SERDAR ŞENGÜL

Bilkent Uni. Advanced Research Laboratories 06800 Çankaya/Ankara •
serdar_sengul@outlook.com.tr • +90 546 559 5922

EDUCATION

Gaziantep University
Gaziantep,Turkey

MSc., Optic and Acoustic Engineer
2021 – cont.

BSc., Optic and Acoustic Engineer
2013 - 2018

EXPERIENCE

UNAM (National Nanotechnology Research Center) / Bilkent University
Ankara, Turkey

Research & Development Engineer
July 2019 – Present

- Thermoreflectance Imaging of the Lasers
- Parity Time Symmetric Lasers Characterization
- High Power Laser Characterization
- High Power Laser fabrication in clean room.
- Clean room experience for the semiconductor laser fabrication. (High Power Laser)
- Photonics devices and applications
- Optical setup installation and sensitive alignment procedure with opto-mechanical parts and geometric optic applications
- Semiconductor lasers tests

SKILLS

Optic

- Optic laboratory responsible
- Geometric optic measurements
- Optical setups building and general optic measurements
- CAT software part design
- Sequential and Non-sequential mode lens and optical systems designs in ZEMAX.

Computer

- ZEMAX
- SolidWorks
- Labview
- Dialux
- MATLAB
- Origin
- MS-Office

Diode Laser Characterization

- Photonics devices characterization
- LIV Measurement
- Far-Field/Near Field Measurement (Thorlabs Scanning Slit Optical Beam Profiler (BP209-VIS/M) / Dataray WincamD Beam Profiler)
- Spectrum measurement (AQ6373B Visible Wavelength Optical Spectrum Analyzer)
- M2 Measurement (Thorlabs M2 Measurement System Extension Set M2MS-AL)
- Packaging lasers (die-wire bonding, MCC adaptor designing, cooling systems of packaging.)

Clean Room Experience

- Clean room machines usage;
- Mask Aligner (Aligner with Nanoimprint Lithography)
- PECVD (Advanced Vacuum Plasma Enhanced Chemical Vapor Deposition)
- E-Beam (E-Beam Evaporator)
- ICP (Inductively Coupled Plasma 615 (Si))
- Box Coater (E-beam, Thermal and Sputter Deposition)
- RIE (Reactive Ion Etching)
- RTP Asher(Oxygen Plasma Cleaning)
- Wire Bonding (K&S 4500 Wire Bonder)
- High Power Laser fabrication full process in clean room.
- Some cleaning steps for lasers. (Piranha, Aqua Regia, Oxygen Plasma)
- Wire Bonding operation for the CC, PTS and High Power Lasers
    - Edge emitting and VCSEL lasers of Near-Field, Far Field, LIV, Spectrum measurements, M2 Measurement and determining its thermal behaviors.
    - Wire bonding for the laser bars.

TURKISH ARMED FORCES
Iğdır, Turkey

Reserve Officer
Jan 2019 – July 2019

FEKA AUTOMOTIVE (Internship)
Bursa/Turkey

Research Intern
Feb – Jun 2018

GAZIANTEP UNIVERSITY OPTIC AND ACOUSTIC ENGINEERING DEPARTMENT Gaziantep, Turkey

Optic laboratory volunteer assistant
Sept 2013 – Jun 2018

ACHIEVEMENTS

2013-2014 Gaziantep University Optic and Acoustic Engineering, Cassegrain Telescope Project.

2016-2017 Gaziantep University Optic and Acoustic Engineering, Wireless Optical Communication.

2016-2017 Gaziantep University Optic and Acoustic Engineering Noise Measurement of Gaziantep University and Noise Mapping.

2016-2017 Gaziantep University Optic and Acoustic Engineering, Room Acoustic Calculation and Measurement with ODEON software.

2017-2018 Gaziantep University ARGETİ Project Market Championship Award.

PUBLICATIONS

- Enes Şeker, **Serdar Şengül**, Khalil Dadashi, Babak Olyaeefar, Abdullah Demir, "Single-mode operation of electrically pumped edge-emitting lasers through cavity coupling of high order modes", Proc. SPIE 11983, High-Power Diode Laser Technology XX, 119830C (4 March 2022); doi: 10.1117/12.2607939
- Kaveh Ebadi, Yuxian Liu, Ali Kaan Sünnetçioglu, Sinan Gündogdu, **Serdar Şengül,** Yuliang Zhao, Yu Lan, Guowen Yang, Abdullah Demir "Multisection waveguide method for facet temperature reduction and improved reliability of high-power laser diodes", Proc. SPIE 12141, Semiconductor Lasers and Laser Dynamics X; 1214104 (2022); doi.org/10.1117/12.2621651
- Yuxian Lıu, Kaveh Ebadi, Ali Kaan Sünnetçioğlu, Sinan Gündoğdu, **Serdar Şengül**, Abdullah Demir, "Elimination of catastrophic optical mirror damage in continuous-wave high-power laser diodes using multi-section waveguides", Proc. Optics Express Vol. 30, No. 18 / 29 Aug 2022 / Optics Express 31539

- Abdullah Demir, Kaveh Ebadi, Yuxian Liu, Ali Kaan Sünnetçioğlu, Sinan Gündoğdu, **Serdar Şengül**, Yuliang Zhao, Yu Lan, Guowen Yang, "COMD-free continuous-wave high-power laser diodes by using a multi-section waveguide method", Proceedings Volume 12403, High-Power Diode Laser Technology XXI; 124030D (2023), doi.org/10.1117/12.2650619

- Abdullah Demir, Enes Şeker, Babak Olyaeefar, Khalil Dadashi, **Serdar Şengül**, Mohammad Hosain Teimourpour, Ramy El-Ganainy, "Single-mode quasi PT-symmetric laser with high power emission" Nature Light: Science & Applications, Light Sci Appl 12, 149 (2023) https://doi.org/10.1038/s41377-023-01175-6

REFERENCES

- Asst. Prof. Dr. Abdullah Demir (Advisor) abdullah.demir@unam.bilkent.edu.tr

  Bilkent University / UNAM (Institute of Materials Science and Nanotechnology

- Dr. Babak Olyaeefar (Postdoctoral Researcher) babak.olyaeefar@ unam.bilkent.edu.tr

  Bilkent University / UNAM (Institute of Materials Science and Nanotechnology)

- Prof. Dr. Ahmet Bingül bingul@gantep.edu.tr

  Gaziantep University / Engineering Physics - Optic and Acoustical Engineering

- Prof. Dr. Ahmet Necmeddin Yazıcı yazici@gantep.edu.tr

  Gaziantep University / Engineering Physics - Optic and Acoustical Engineering

- İhsan Çaylı Physic/Optical Engineer ihsan.cayli@outlook.com

  ASELSAN - Test System, Process Design Management (TSPDM)

- Murat Çalık Production Engineer muratcalik@aselsan.com.tr

  ASELSAN (REHIS) – Microwave Hibrid Modul Production Management